Chapter 3

Radiogenic Heat Generation in Western Australia — Implications for Geothermal Energy

Mike F. Middleton

Additional information is available at the end of the chapter

http://dx.doi.org/10.5772/61963

Abstract

The chapter reviews heat generation in crystalline rocks and influences on overlying sedimentary basins in Western Australia (WA). Regions of elevated thorium and uranium will cause elevated heat generation, which in turn can cause elevated heat flow. Western Australia hosts several large sedimentary basins with the potential for hot sedimentary aquifers (HSAs). These include the Perth, Carnarvon, and Canning basins. Parts of these basins are underlain by crystalline rocks that contain high levels of heat-generating elements, such as uranium, thorium, and potassium. Also, the Pilbara Craton, which contains both sedimentary and crystalline rocks, that entertains a number of active mines, which may benefit from geothermal energy, is investigated. Further, the southern part of the Perth Basin (Vasse Shelf), which is underlain by crystalline rocks with elevated concentrations of thorium and uranium, is shown to possess higher than usual temperatures. From observations, and geothermal modeling, it is concluded that the Perth Basin has a high potential for medium- to low-temperature geothermal energy developments. In other parts of Western Australia, the Carnarvon Basin has elevated temperatures in artesian groundwater. Heat flow in the Canning Basin is briefly reviewed; this basin has some geothermal potential, but it is far from the major population centers.

Keywords: Radiogenic heat, Uranium, Thorium, Potassium, heat flow

1. Introduction

The information presented in this study reflects the view in Western Australia to move toward mechanisms for sustainable energy into the future. The Western Australian legislative framework supports this view, and continuous studies have been carried out since 2008 to implement this vision into the future. The initial formal Western Australian governmental view was to use geothermal energy for electricity generation, and legislation was formulated

to accommodate this. By late 2014, it became apparent that geothermal energy in Western Australia was taking a different path. The chapter focuses, both formally published works and less formal studies, on radiogenic heat generation within rocks in Western Australia and their contribution to heat flow, elevated temperatures, and geothermal energy potential. It adopts the approach that heat flow from basement (essentially crystalline) rocks beneath sedimentary basins will elevate temperatures within the sedimentary basin, and thus create a natural reservoir of hot fluids in the sediments that can be used for geothermal energy purposes. These are referred to as hot sedimentary aquifers.

The connection between radioactive elements in the earth and heat generation has been known for many years. Among many, the following workers have developed this science [1–3], and in specific reference to Australia [4–7]. About this period, an increasing awareness was growing for the potential need for geothermal energy in the Australian energy mix, and a landmark book was published by Beardsmore and Cull [7]. Studies were undertaken by Geoscience Australia, the national geoscience survey organization in Canberra [8–10]. In Western Australia, one of the significant early workers to recognize that geothermal energy may be viable in the state was by Bestow [11]. In his study, Bestow [11] recognized parallels of Western Australian basins to the Paris Basin and the need to achieve temperatures in the vicinity of 65–85 °C. At this early stage, Bestow also clearly recognized that the geothermal potential in Western Australia was best based around the concept of hot sedimentary aquifers, rather than either the engineered geothermal systems (EGSs) being advocated elsewhere in Australia [12,13] or the more commonly exploited volcanogenic heat sources.

Early work on heat flow and radiogenic heat production was carried out by Jaeger [4], Sass et al. [5], Middleton [6], Cull and Denham [14], and Cull [15]. These studies identified the background to understanding heat flow and heat generation in Western Australia. Perhaps rather more by serendipity than by intention, the study by Jaeger [4] identified a rather unique site in the "Wheat Belt" of Western Australia (Figure 1). This site was in a granite quarry near the small town of Doodlakine, and returned a heat generation value of about 21.9 heat generation units (hgu; 1 hgu = 0.418 μW m^{-3}) at the surface and 21.2 hgu as an average of 30 samples from an associated bore hole. This translates to 9.15 μW m^{-3} in SI units. At the time, this was the largest heat generation value published for a Western Australian granitoid (a term used herein to refer to a felsic igneous rock with largely granitic mineralogy). More recent work on heat generation in Western Australia was carried out by Middleton [16], Middleton and Stevens [17], and Middleton et al. [18]. During these studies, the Doodlakine site was revisited and now initially reported; surface measurements of heat generation of the granite near the original measurements published by Jaeger [4] were made, using an RS-125 gamma-ray scintillometer (see below for description of the technique). Twelve measurements were made on the granite outcrop, near where Jaeger (1970) carried out his investigation, and these yielded a mean heat generation of 8.5 μW m^{-3} (20.3 hgu used by Jaeger [4]). This is a good agreement, given slightly different assumptions made for conversion of uranium (U), thorium (Th), and potassium (K) concentrations to heat generation, made by Jaeger [4] as compared with Middleton [16].

http://dx.doi.org/10.5772/61963

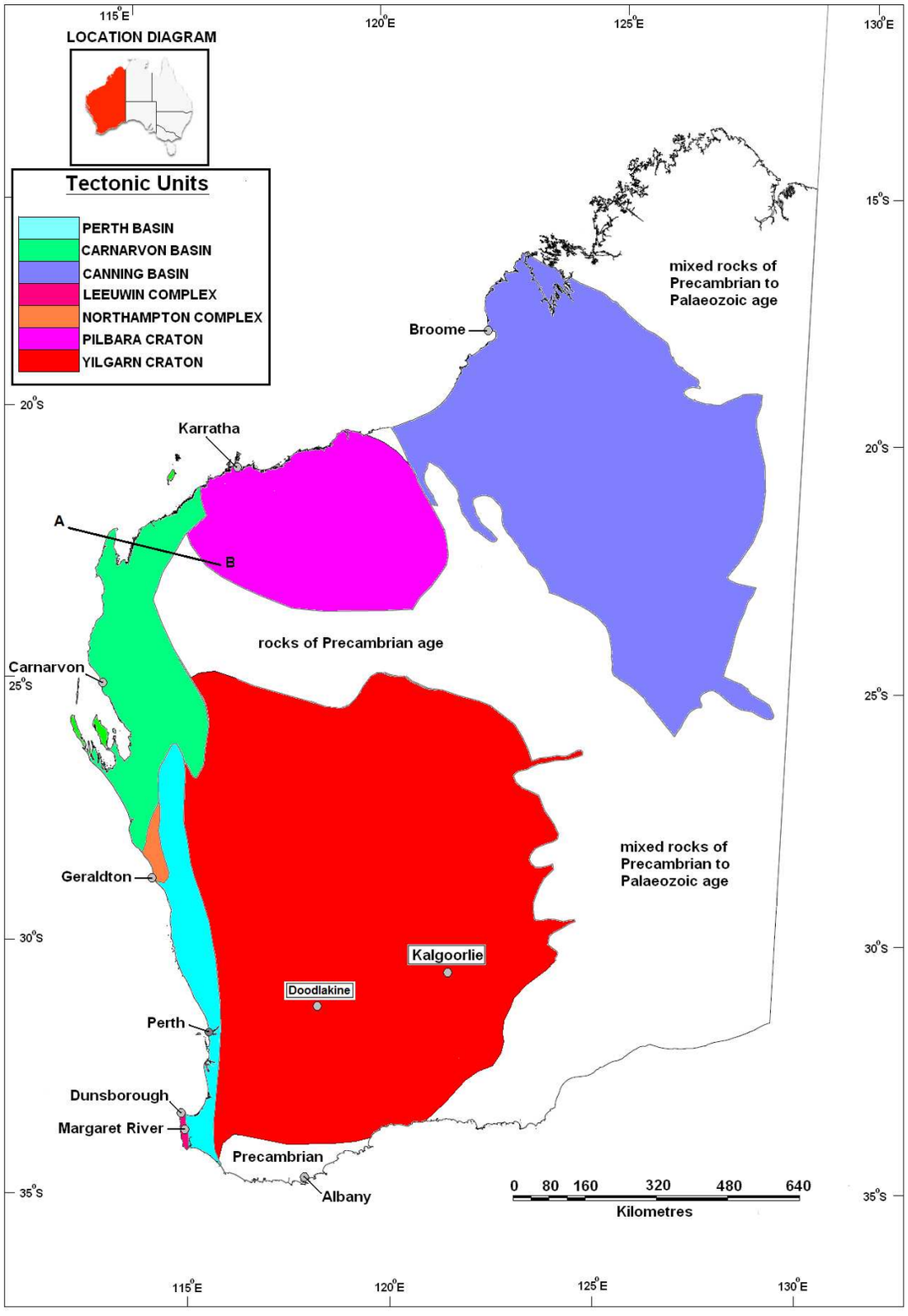

Figure 1. WA map showing tectonic provinces. Note that the Doodlakine location is halfway between Perth and Kalgoorlie.

Uranium distribution, as with Th distribution, in Western Australia is poorly known at depth. However, a reasonable knowledge of surface U distribution is known from airborne radiometric data compiled in the "uranium merge" and "thorium merge" maps of the state produced by the Geological Survey of Western Australia [19]. The U and Th merge maps are shown in Figure 2. It must be recognized that these maps have limitations because of the attenuation of radiation, due to many effects, for example, the distance from surface radioactive source rocks to the sensor in the aircraft, time of day of acquisition, the limitations (because of different instrumentation and calibration) in the merge process for various survey datasets, and the difference in surface geology across the state [20,21]. From the maps, it is observed that Th concentration (parts per million, ppm) is generally higher than the U concentration. Thorium to uranium ratio (Th/U) has been reviewed by Middleton et al. [18] for various surface locations (Table 1). It should be noted that the surface U and Th concentrations from airborne measurements are commonly lower than surface measurements of concentration, because of the environmental effects commonly observed in deriving U and Th from the surface "merge" maps [20,21]. From the data in Table 1, the Th/U ratio showed a variation between 2.0 and 13.0 for outcrop rocks. Uranium and thorium are often concentrated in deeply emplaced felsic igneous (granitoid) rocks. However, these elements can also be concentrated in sedimentary rocks. In recognizing this, some surface measurements of U and Th in sedimentary basins may be higher than normal due to sedimentary depositional and enrichment processes.

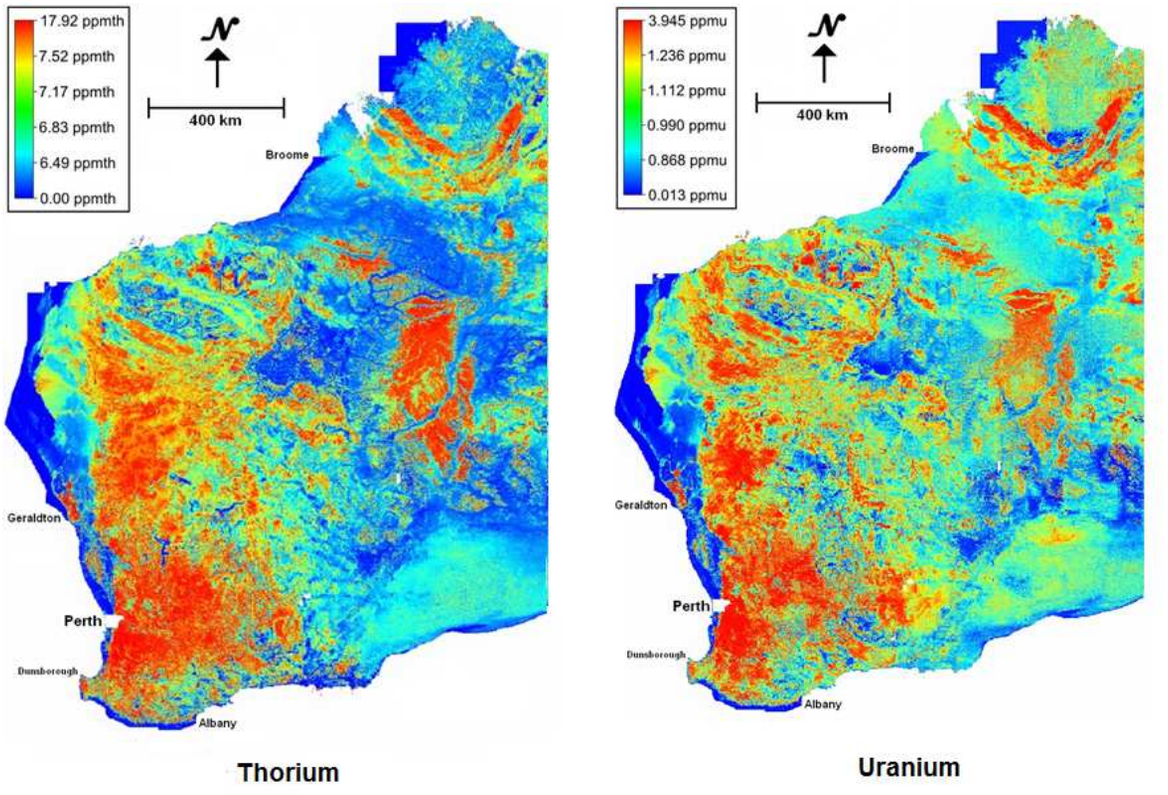

Figure 2. Map with surface U and Th surface distribution in WA. These are based on "merge maps" produced by Brett [19] for the Geological Survey of Western Australia.

http://dx.doi.org/10.5772/61963

LOCATION	μR/hr	A_o (μW/m³)	Th (ppm)	U (ppm)	K(%)	Comment
Sugarloaf 1	480.5	9.9	108.4	6.0	7.4	Leeuwin (granitoid)
Sugarloaf 2	130.3	2.2	21.3	1.3	3.8	Leeuwin (granitoid)
Gracetown N	251.0	4.2	49.1	0.7	6.3	Leeuwin (granitoid)
Gracetown S	154.7	2.6	24.4	1.8	4.6	Leeuwin (granitoid)
Leeuwin LH	217.7	3.9	37.8	2.8	5.6	Leeuwin (granitoid)
Wagon Wheel	257.0	4.8	46.8	3.3	6.2	Leeuwin (granitoid)
Meelup Pk 1	600.8	15.7	168.0	12.6	6.2	Leeuwin (granitoid)
Meelup Pk 2	485.3	12.3	140.9	7.6	4.9	Leeuwin (granitoid)
Meelup Pk 3	843.0	40.1	178.9	32.3	6.3	Leeuwin (enrichment)
Point Picouet	147.1	2.2	20.4	0.1	7.0	Leeuwin (granitoid)
Cowaramup	389.3	11.5	82.5	20.3	4.4	Leeuwin (granitoid)
Farquhar Rd	574.0	15.2	147.2	18.7	0.4	S. Perth B (sediment)
Carbunup 1	59.5	1.6	13.3	2.6	0.2	S. Perth B (sediment)
Carbunup 2	49.0	1.4	10.1	2.7	0.1	S. Perth B (sediment)
Rosa Brook 1	479	12.0	129.7	10.7	0.1	S. Perth B (enrichment)
Rosa Brook 2	198	4.9	56.2	3.7	0.02	S. Perth B (enrichment)
Stoneville	200.1	4.5	32.6	6.9	3.9	Darling R (granitoid)
Ashenden Rd	241.5	5.4	44.7	7.3	3.8	Darling R (granitoid)
Golden View 1	242.6	5.9	36.8	11.0	4.1	Darling R (granitoid)
Golden View 2	255.7	5.7	42.1	9.0	4.5	Darling R (granitoid)
Darlington	138.6	3.3	20.7	6.1	2.5	Darling R (granitoid)
Chalet Rigi	369.5	10.2	55.7	22.7	3.8	Darling R (granitoid)
J Forrest Pk1	309.8	8.0	45.0	17.0	4.0	Darling R (granitoid)
J Forrest Pk 2	245.3	6.0	42.6	10.1	3.5	Darling R (granitoid)
J Forrest Pk 3	285.5	7.3	43.2	14.7	4.2	Darling R (granitoid)
J Forrest Pk 4	279.0	7.3	40.1	15.8	3.7	Darling R (granitoid)
Parkerville	224.3	5.8	42.2	9.6	3.8	Darling R (granitoid)
Canning Dam	176.3	4.3	30.2	7.3	2.6	Darling R (granitoid)
Mundaring 1	3.6	0.9	7.6	1.5	0.2	Darling R (sediment)
Mundaring 2	4.1	1.3	8.1	2.1	1.9	Darling R (sediment)
Mundaring 3	25.1	6.4	68.6	6.0	0.2	Darling R (laterite)
Doodlakine	359.0	8.2	76.7	10.4	4.0	Central Yilgarn (gr.)
Cunderdin	297.6	6.3	65.2	5.0	4.5	Central Yilgarn (gr.)
Goongarrie	7.5	1.1	7.7	1.9	2.6	Central Yilgarn (gr.)

Table 1. Western Australian RS-125 measurement campaign for U, Th, K & A_o for the years 2011 and 2015.

Potassium usually has a different genesis to U and Th. It is a very commonly occurring element in the earth's crust. The abundance (concentration) of K in most igneous rocks is commonly observed to be about 2–6%, and it also occurs abundantly in many sedimentary rocks. Beardsmore and Cull [7] have discussed the specific abundance of the radioactive isotope (K-40) within normal potassium distributions in rocks. The surface K "merge" distribution map [19] can be misleading, as the K concentrations tend to follow recent sedimentary depositional features, such as seasonally dry riverbeds. In such deposits, the time of year of that an airborne radiometric survey was acquired has implications for interpretation of the observed K concentration [20–22]. Further, as will be seen in the following sections, the contribution of K to radiogenic heat generation is usually less than the contribution of U and Th [7,16,23].

In this review, surface-based geophysical or laboratory measurements of U, Th, and K are emphasized rather than airborne measurements. This is because surface-based (on-the-ground) measurements of outcropping rocks tend to be more directly indicative of the particular rock type being investigated, rather than a "bulk" estimate of the chemistry of the rocks being sampled by an airborne survey. This will be discussed further below.

2. Theory

This section reviews the basic, but well-known, concepts to understand heat generation, heat flow, and simple temperature distributions with the earth's crust.

2.1. Heat flow and temperature due to heat generation in a radiogenic layer

Heat flow at the surface on the earth (Q_s) over a series of n layers with internal heat generation and stable tectonic environment can be determined by the equation

$$Q_s = Q_b + A_1H_1 + A_2H_2 + \ ... \ + A_nH_n, \tag{1}$$

where Q_b is the heat flow from the base of the n layers being considered, typically the upper mantle, A_1 is the heat generation in layer 1, H_1 is the thickness of layer 1, A_2 is the heat generation in layer 2, H_2 is the thickness of layer 2, A_n is the heat generation in layer n, and H_n is the thickness of layer n.

Temperature within a surface layer of thickness L, and uniform heat generation of A_0, is shown by Carslaw and Jaeger [24], described by the equation:

$$T = \left[\frac{A_0 z}{2K}\right](2L - z) + \frac{Q_b z}{K} + T_s, \tag{2}$$

http://dx.doi.org/10.5772/61963

where T is the temperature, z is the depth of observation, K is the thermal conductivity, T_s is the mean annual surface temperature, and Q_b is the heat flow at the base of the layer. The geometry applicable to this equation is shown in Figure 3, and this equation can be applied to estimate the temperature versus depth in a granite batholith with uniform radiogenic heat generation.

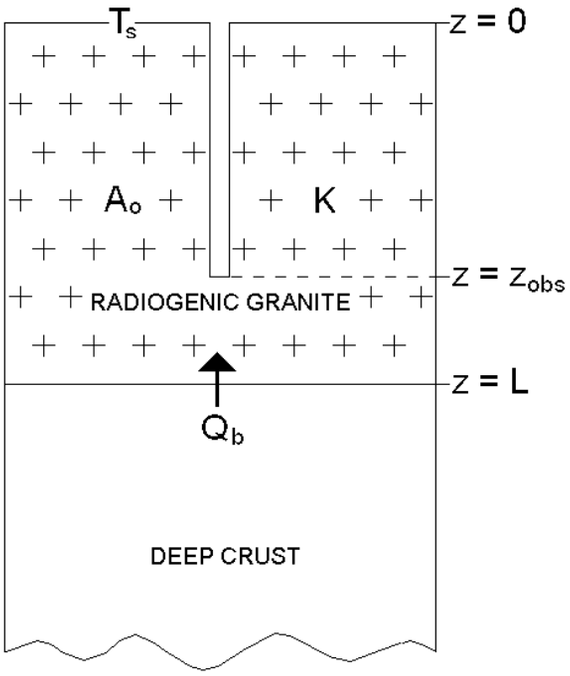

Figure 3. theory for temperature model. Note that the same modeling geometry is used for relatively thin enrichment layer models in section 7. In the latter case, the radiogenic granite layer is a layer where U- and Th-rich fluids have been rapidly emplaced due to chemical alteration processes, largely due to weathering and erosion.

The more general time-variable equation describing the gradual rise in temperature due to thermal adjustment of the emplacement of a layer of thickness L at an initial time of t=0 is given by Carslaw and Jaeger [24] for $0 < z < L$:

$$T = \left[\frac{\alpha A_0 t}{K}\right]\left[1 - 4i^2\mathrm{erfc}\left(\frac{z}{\tau}\right) + 2i^2\mathrm{erfc}\left(\frac{L+z}{\tau}\right) - 2i^2\mathrm{erfc}\left(\frac{L-z}{\tau}\right)\right] + T_0\mathrm{erf}\left(\frac{z}{\tau}\right) + \frac{Q_b z}{K}, \quad (3)$$

where T is the temperature, z is the depth, t is the time, α is the thermal diffusivity, K is the thermal conductivity, A_0 is the heat generation, T_0 is the initial temperature of layer at $t = 0$, Q_b is the heat flow at the base of layer, erf(x) is the error function, erfc(x) is the complimentary error function [1 − erf(x)], i^2erfc(x) is the second integration of the error function, and $\tau = (4\alpha t)^{1/2}$. The temperature modeling below is largely based on these three equations. A theoretical case, based on Eq. (3), where a radiogenically enriched layer of variable thickness occurs, by chemical alteration processes, at the earth's surface is also investigated in Section 7.

The case of sedimentary layers overlying a radiogenic granite is also important. This situation has the potential to cause a "thermal blanketing effect," where the overlying sediments possess significantly lower thermal conductivity than the underlying rocks. In many cases, this has been shown to create anomalously high temperatures within the upper sedimentary sequence. Such cases have been treated theoretically by Carslaw and Jaeger [24]. In the Western Australian perspective, the "thermal blanketing" effect was investigated in the case of a geothermal (temperature) anomaly in the northern Perth Basin (Gillingarra anomaly) and is discussed below. This investigation showed that the wavelength of the observed heat flow anomaly was too low (and magnitude too high) to accommodate a radiogenic heat source from an estimated 10-km basement depth.

2.2. Heat generation from U, Th, and K

Studies of radiogenic heat generation from the decay of unstable isotopes of U, Th, and K have been summarized by Kappelmeyer and Haenel [23], Jessop [25], Beardsmore and Cull [7], and Middleton [16]. The generalized relation [16] used for the present study is

$$A_0 = \left(0.26\right)\left(\text{U ppm}\right) + \left(0.07\right)\left(\text{Th ppm}\right) + \left(0.1\right)\left(\text{K \%}\right), \tag{4}$$

where A_0 is the heat generation, (U ppm) is the concentration of uranium in ppm, (Th ppm) is the concentration of thorium in ppm, and (K %) is the concentration of potassium in percent. The relationship used in Eq. (4) is consistent with that of Beardsmore and Cull [7]. It is recognized that by using these constants in Eq. (4), the density of all rocks is assumed to be a constant value of 2700 kg m^{-3} (as is similarly assumed in the example of Beardsmore and Cull [7]). Essentially, this assumption represents a generalized conversion formula.

2.3. Field measurements with an RS-125 gamma-ray spectrometer

For studies reviewed in this chapter, many of the sites measured for U, Th, and K assay were obtained using an RS-125 gamma-ray spectrometer. The RS-125 instrument is calibrated, via "assay mode", to provide an approximation of U, Th, and K concentrations in a half-space being sampled. The manufacturer indicates that an instrumental error of about 10% is incurred in the RS-125 in the assay mode, due to the programmed calibration matrix. The volume sampled is assumed to be a perfect half-space, and variations from this perfect half-space can also cause some errors in the assay determination. However, observation locations were chosen so as to minimize this type of error. The manufacturer's specifications of the RS-125 spectrometer indicate that the instrument reflects a sample area of a radius of approximately 1 m in the half-space (Figure 3).

Calibration procedures were carried out prior to, and during, the field acquisition with the RS-125. An important factor for calibration is the sample time of each measurement. In determining this, the manufacturer asserts that the calibration matrix, which is used to optimize the spectral definition of the three isotopes, is designed to provide the minimum error (< 5%) for sample times of approximately 4 minutes. However, this has to be balanced against

http://dx.doi.org/10.5772/61963

the requirement for long sample times (often over many hours) for rocks with low U, Th, and K concentrations, as expected in many of the granites being investigated. It was finally decided to base all measurements for studies reported in this review to be 5 minutes [16]. Further, the RS-125 field assays were compared with U, Th, and K assays obtained by laboratory measurements for sample sites in the Leeuwin Complex in the southwest of Western Australia, and good correspondence was observed (Figure 4).

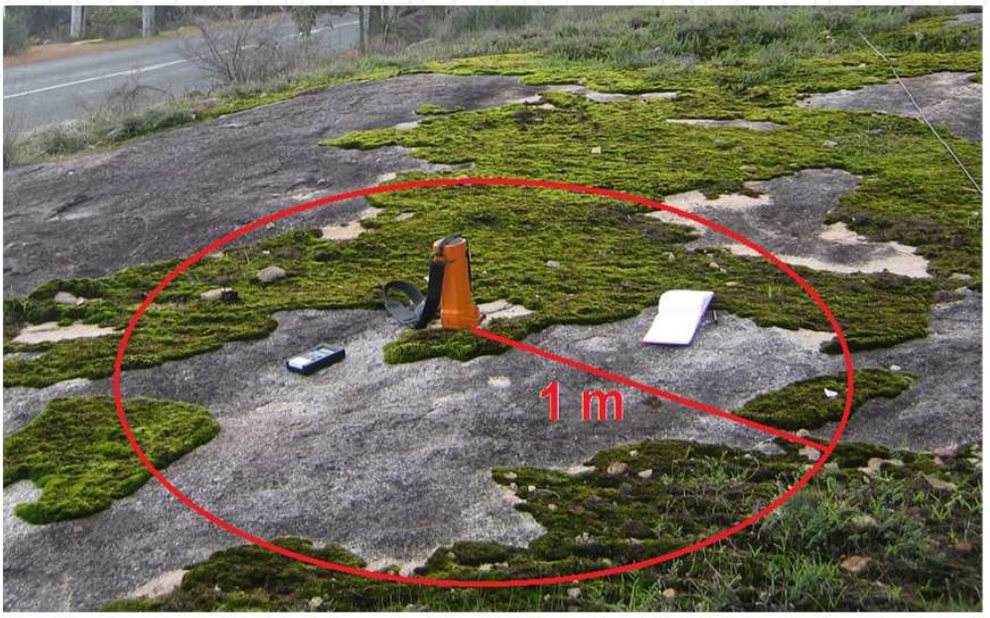

Figure 4. A diagram showing the RS-125 sampling zone, which is essentially a 1-m-radius hemisphere below the earth's surface.

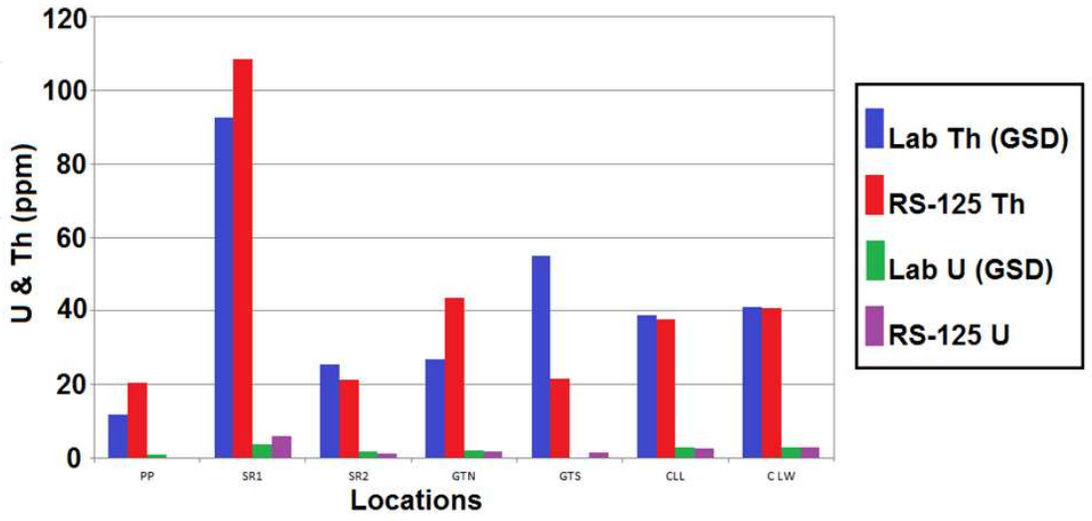

Figure 5. Correlation of RS-125 to laboratory assays for Leeuwin Complex samples.

2.4. Heat generation derived from gamma logs

Ryback [26] and Bücker and Ryback [27] proposed empirical equations to determine heat generation (A_0, μWm^{-3}) from wire-line gamma-ray (GR) logs run in (petroleum and sometimes mineral) exploration wells or boreholes. The Bücker and Ryback [27] correlation appears to be superior to the earlier correlation by Ryback [26], and is expressed as

$$A_0 = 0.0158\ (\mathrm{GR}) - 0.0126\,, \tag{5}$$

where A_0 is the heat generation (in units of μWm^{-3}) and GR is the logged gamma-ray value in API (American Petroleum Institute) units. A gamma-ray API is defined, and further discussed in relation to other radioactivity measurement units, in Society of Petroleum Engineers (SPE) [28]. When looking at gamma-ray measurements greater than 20 API units, this equation simplifies to $A_0 \approx 0.0158$ (GR). For this study, it is assumed that $A_0 = 0.0158$ (GR).

Beardsmore and Cull [7] investigated this relationship with regard to the East Yeeda 1 well from the Canning Basin in Western Australia. They derived a relationship between heat generation and the gamma-ray and density logs from this well, which had total count and spectral gamma-ray logs. These workers derived a relationship between the heat generation and the two wire-line-log values to be

$$A_0 \approx 0.005\ (\mathrm{GR})\ (\mathrm{RHOB}), \tag{6}$$

where RHOB ($g\ cm^{-3}$) is the bulk density and GR (API units) are the readings from the wire-line log. The authors suggest that an uncertainty in A_0 is about ± 0.5 $\mu W\ m^{-3}$. These workers place the caveat that this relationship may be local correlation, rather than a general relationship. If we assume a general rock density of 2700 $kg\ m^{-3}$, then the Beardsmore and Cull relationship becomes

$$A_0 \approx 0.014\ (\mathrm{GR}). \tag{7}$$

On the basis of these considerations, Eqs (5) and (7), heat generation may be in a very general sense correlated to the wire-line log gamma-ray value by a relationship represented by the range 0.014 (GR) < A_0 < 0.016 (GR), with GR in API units and A_0 in $\mu W\ m^{-3}$.

From 2011 to 2015, a series of studies was carried out with a commercial gamma-ray spectral scintillation detector, RS-125 instrument, as described below. This instrument was used to measure many of the heat generation estimates reported in this study [16,18]. It is of importance to establish how this instrument performs, and provides results, consistent with other radioactive measuring instruments. Since 2011, the results shown in Figure 6 have been accumulated, which can provide an approximation of dose rate (DR; as reported by the instrument) with respect to uranium (ppm), thorium (ppm), and potassium (K). This correla-

http://dx.doi.org/10.5772/61963

tion can provide a correlation of dose rate to heat generation via Eq. 4. Correlations, according to the data in Figure 6, can be established between DR and A_0, with heat generation values (A_0) being determined according to Eq. (4). Regression curves have been established for (1) DR total and (2) DR <300 μR/hr. It is believed that DR (μR/hr) < 300 may be more appropriate for correlation studies, because of the nonlinearity of the DR versus A_0 relationship above the value of 300 μR/hr. In the case of all the data being incorporated, a second-degree polynomial curve DR = 0.6292 $(A_0)^2$ + 47.186 (A_0), with regression coefficient of R^2 = 0.9254, is found to provide the best match (Figure 6).

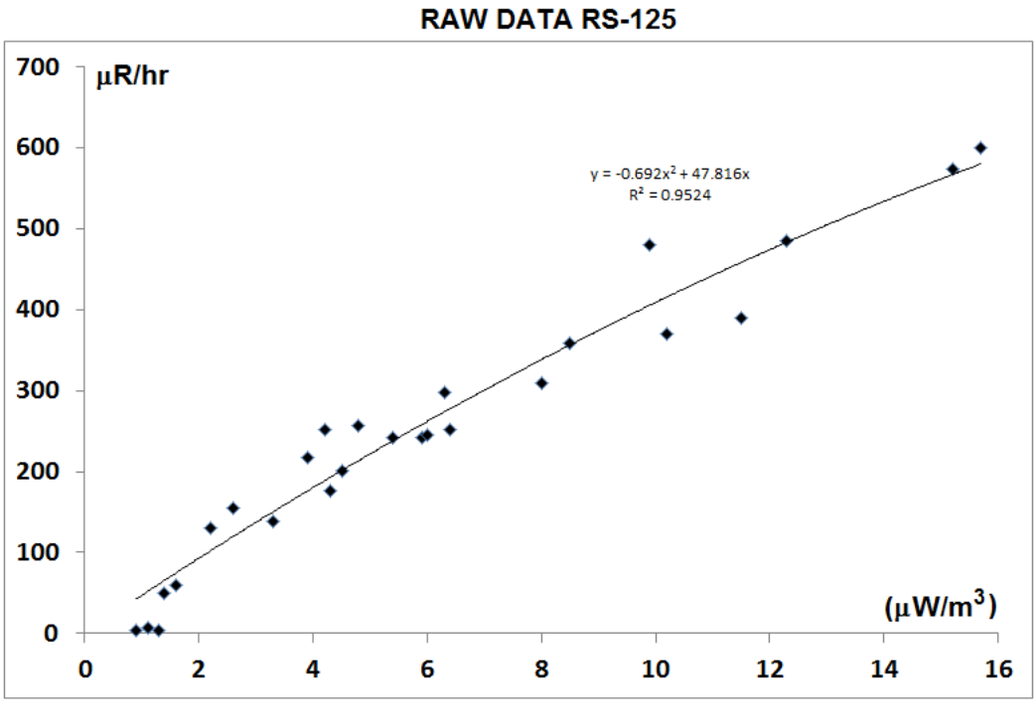

Figure 6. Correlation between RS-125 dose rate in (üR/hr) and heat generation (μW/m^3) from the data derived by field measurements [16,17].

In the special case of DR being < 300 μR/hr, a regression match is found to be DR = 43.21 (A_0), with a regression coefficient of R^2 = 0.8866. In this case, an intercept at zero is also assumed. The observed data for A_0 less than about 1.3 μWm^{-3} (DR < about 15 μR/hr) appear to be showing a limitation in the calibration of the scintillation crystal to accurately measure the uranium, thorium, and potassium elemental concentration spectra, and more research is required to look into why this is happening. Despite the concerns of the calibration of the RS-125 crystal at low U, Th, and K concentrations, the author believes, that sufficient confidence can be placed in the data for DR >15 μR/hr, that an acceptable correlation between DR and A_0 can be sustained to be DR = 0.43.21 (A_0). Assuming the SPE correlation between DR and API gamma-ray measurements is DR = 0.67 API units [28], the data found by Middleton [16] indicate a correlation of DR ≈ 0.0155 (GR). This correlation is very close to the Bücker and Ryback [27] approximation.

It is proposed that an approximate conversion factor for GR (API units) to A_0 (μWm^{-3} units) for this investigation to be

$$A_0 = 0.015\ (\mathrm{GR})\ . \tag{8}$$

This equation is the mean of the Bücker and Ryback [27] and Beardsmore and Cull [7] approximations. Some estimates of heat generation, derived from this equation, of the gamma-ray response of basement rocks observed in wire-line logs from the Perth Basins are shown below.

3. Perth basin

The Perth Basin lies in the southwest corner of Western Australia (Figure 1). It contains sediments of Phanerozoic age, which are surrounded by crystalline granitoid and metamorphic rocks of the Yilgarn Craton, Leeuwin Complex, and Northampton Complex (Figure 1). The Perth Basin will be treated in three parts: the southern Perth Basin [29], the central Perth Basin [30–32], and the northern Perth Basin [33].

3.1. Southern perth basin

Heat generation in the granites of the Leeuwin Block, which immediately crops out to the west of the Vasse Shelf, may have relevance for the exploration for geothermal energy "hot spots" in the Vasse Shelf sediments (Figure 1). The significance of measuring heat generation in the Leeuwin Complex is that it is expected that these rocks underlie the elements of the Perth Basin immediately to the east of these outcropping sediments. The elements of the Perth Basin in question are the Vasse Shelf sediments (largely of Permian age) and the deeper and thicker Bunbury Trough sediments (largely of Cretaceous to Permian age) [29]. It is uncertain if the Leeuwin Complex crystalline rocks extend under the Bunbury Trough, which has been described geologically by Crostella and Backhouse [29].

Western Australia has several regions where hot granitoids are known to occur in outcrop. The locations of high radioactivity rocks, including hot granitoids, can initially be detected by airborne radiometric surveys. These data have been acquired for Western Australia through a number of cooperative projects between the Geological Survey of Western Australia and Geoscience Australia, and maps showing these data are publically available. The Vasse region was flown in 2011. The U concentration map for the northern part of the Vasse Region, derived from this survey, is shown in Figure 2a, and the Th map for the same region is shown in Figure 2b. A ground-truthing survey was carried out by the members of the Petroleum Division of the Department of Mines and Petroleum in May 2013. This survey used a RS-125 gamma-ray spectrometer to obtain surface values of U, Th, and K to compare with the airborne data. Middleton [16,34] carried out a similar study to investigate geothermal heat generation for the Darling Range granitoids. Surface sampling of granitoids of the Leeuwin Complex was

http://dx.doi.org/10.5772/61963

previously carried out by the Geological Survey of Western Australia and Geoscience Australia, and these sites were also revisited during 2011 and 2012 to compare the spectrometer values to those obtained by the previous laboratory-based measurements of U, Th, and K (main locations shown in Figure 8). The U, Th, and K concentrations in the granitoids can be converted into approximate radiogenic heat generation using Eq. (4); see Figure 7.

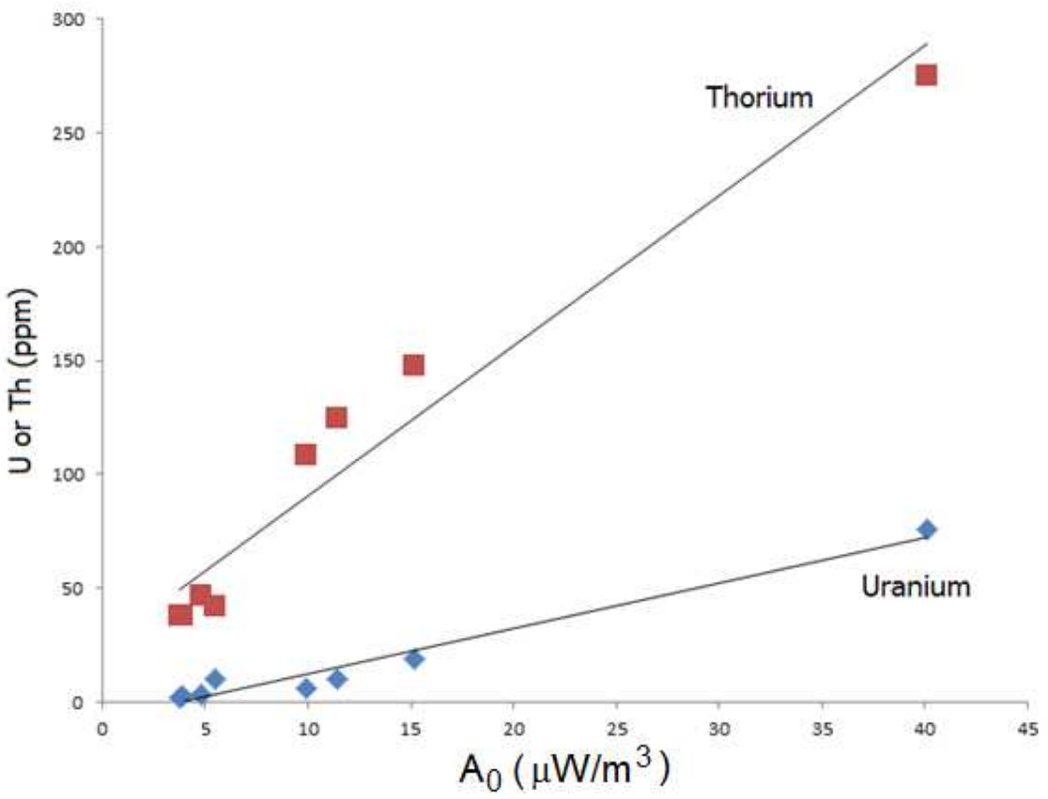

Figure 7. Correlation of U or Th concentration to heat generation, using Eq. (4).

Previous works [4,5,16,34,35] have been carried out on heat generation in granitoids of the western part of the Yilgarn Craton. The heat generation of outcropping hot granites in the Yilgarn Craton has been measured in the range of 1–10 μWm^{-3} and is similar to published values for the Cooper Basin Hot Dry Rock (HDR) granites (ca. 10 μWm^{-3}) [6]. Some previous heat generation values were published for the Leeuwin Complex by Middleton and Stevens [17], although U, Th, and K analyses have been measured by laboratory techniques from outcrop samples for selected locations (see Figure 7). More recent heat generation values have been acquired in the northern part of the Leeuwin Complex and are herein reported.

Table 1 shows the mean U, Th, and K concentrations (measured with at least three repeats) at the 16 localities in this Leeuwin and south Perth Basin reviewed in this study. The elemental abundances observed at these sites were converted to heat generation in units of μWm^{-3} using the factors in Eq. (4). Table 1 shows the relationship between U, Th, K and heat generation (designated as A_0). The table indicates that the observed mean heat generation at the locations

investigated ranged between 3.8 μWm^{-3} and 40.1 μWm^{-3} throughout the Leeuwin Complex region. The heat generation data exhibit a good linear relationship between U and Th concentrations. The very high U and Th concentrations, and calculated heat generation of 40.1 μWm^{-3}, at the Meelup Park anomaly location (MP in Figure 8) near Dunsborough are indeed anomalous, which was investigated because of the high airborne radiometric signals (see Figures 8–10). The reason may be due to the concentration of these elements in a thin laterite or gravel layer residing on the top of a hot underlying granite body. No obvious outcrop of the underlying granitic rocks was observed during the survey at this locality.

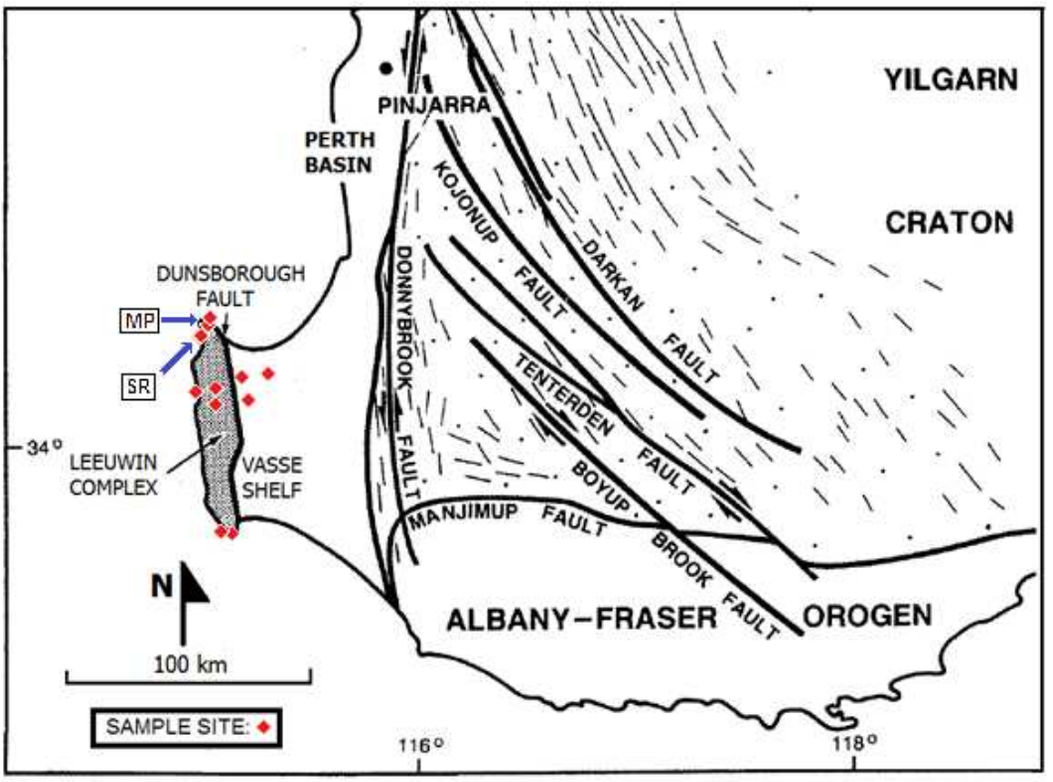

Figure 8. South Perth Basin structural and other tectonic elements.

The airborne signature suggests that the underlying hot granite may have an areal extent of about 5 km^2. Figure 11 shows the thorium anomalies superimposed on the aeromagnetic data at the Meelup Park location. The anomalous thorium appears to be located in a low magnetic region in the range of −50 to −200 nT (green to light blue in Figure11). The low magnitude of the magnetic signature of the thorium-rich regions implies that the thorium may be located in low magnetic crystalline rocks. This tends to suggest that the thorium (and uranium) may be associated with the more felsic rocks in the Leeuwin Complex, which is also supported by evidence from the Sugarloaf Rock locality. The Sugarloaf Rock locality is located on the coast about 3 km south of Cape Naturaliste (see Figure 8). Laboratory measurements by the Geological Survey of Western Australia indicate at least two igneous rock suites at the locality: (a) with U ~3.9 ppm and Th ~92.6 ppm and (b) U ~1.7 ppm and Th ~25.4 ppm. Surface

http://dx.doi.org/10.5772/61963

measurements with the spectrometer yielded that (a) U ranged between 3–8.5 ppm and Th ~108 ppm for an observed felsic suite of rocks and (b) U ~1.3 ppm and Th ~21 ppm for a mafic suite. It should be noted that the felsic suite of igneous rocks are expected to have a low magnetic signature and the mafic suite a high magnetic signature. Measurements at this site support the observations at Meelup Park ("MP" in Figure 8) that the low-magnetic rocks seem to possess a higher concentration of radioactive elements than do the high-magnetic rocks.

A simple 1D model [24] is used to determine the temperature at depth in sediments, which are underlain by a granitic body with uniform heat generation and limited depth extent. The main unknown parameters in this modeling exercise are heat generation within the layer of hot granite (A_0) and its thickness (L). The other parameters, such as thermal conductivity (K), basal heat flow (Q_b), and surface temperature (T_s), are relatively well known [4,35,36], and commonly observed values have been assumed (see Table 2). Several cases with different heat generation and depth extents of hot granites are modeled to investigate temperatures at depth within the western part of the Vasse Shelf. Granitoid bodies with depth extents of 2000, 3500, and 6000 m are considered for this modeling. Heat generation is assumed to vary between 4 and 20 μWm^{-3}. Figure 12 shows temperature versus depth for each of the four cases with corresponding parameters shown in Table 2. The results suggest that temperatures at 3000-m depth in the Vasse Shelf may have temperatures as high as 180 °C, if underlain by a very radioactive granitoid A_0 (> 20 μWm^{-3}) of sufficient thickness (> 6000 m).

PARAMETER	VALUE						
CASE 1	CASE 2	CASE 3	CASE 4	CASE 5	CASE 6	CASE 7	
A_o (μWm^{-3})	4	10	20	4	10	20	8
K ($Wm^{-1}K^{-1}$)	3	3	3	3	3	3	3
L (km)	2	2	2	6	6	6	3.5
Q_b (mWm-2)	26.3	26.3	26.3	26.3	26.3	26.3	26.3
T_s (°C)	20	20	20	20	20	20	20

Table 2. Parameters used in south Perth Basin temperature modeling.

It is worth noting that the hydrogeological study by Wharton [37] reported temperatures within the sediments in the range of 38–40 °C at approximately 1000-m depth. The modeled temperatures in Figure 12 are consistent with the temperatures reported by Wharton [37] for cases 2, 3, 4, and 7 in Table 2. For example, the average case of a radiogenic-rich granitoid with a thickness of 3500 m and heat generation of 8 μWm^{-3} can satisfactorily yield the temperatures observed in the study by Wharton [37], as can a granitoid of thickness of 2000 m and heat generation of 20 μWm^{-3}. Interestingly, in the former case, the temperature extrapolated to 5000 m will be 111°C and 133 °C in the latter case. However, it is unlikely that sediment thicknesses of 5000 m exist in the part of the Vasse Shelf.

3.2. Central Perth basin

3.2.1. Darling range

The Darling Range is a physiographic feature that typifies part of the western margin of the Yilgarn Craton in the southwest of Western Australia. It is dominated by the Darling Fault (Figure 1), which separates the Yilgarn Craton from the Perth Basin [30,32,38,39], and is one of the longest fault zones in the world, extending for about 1000 km. In the vicinity of Perth, the Darling Fault is expressed as a surface scarp of about 300 m, but the subsurface expression of the fault zone on seismic reflection data [40] is observed to extend to over 20 seconds two-way time (approximately 50 km). Most importantly, it is not known if the same rocks that comprise the Yilgarn Craton underlie the Perth Basin, as it is interpreted as a zone of major continental collision and orogenesis. Commonly within the Craton, there is an upper laterite (Regolith) profile that has been formed on the Darling Range granitoids and associated igneous lithologies. In many places, the upper laterite profile has been removed by erosion, generally in incised valleys, and in those places relatively fresh granite is exposed [40,41]. Tertiary channels also occur within the regolith in the Darling Range, and these have also been investigated for surface U, Th, and K (Table 1). Field measurements of abundance of naturally occurring radiogenic isotopes were made in order to estimate radiogenic heat generation of granitoids in the Darling Range region of the Yilgarn Craton. Fifteen locations are reported from this region (Table 1). The field measurements on outcropping granitoids, laterite, and tertiary channel sediments indicate a range of heat generation between 3.3 and 10.2 $\mu W\ m^{-3}$.

An alternative approach to evaluating heat generation is to use Eq. (4) to estimate U, Th, and K concentrations from calibrated airborne radiometric data, which was investigated by Middleton [16]. This is now reviewed. A heat generation map (Figure 6), based on airborne radiometric data, was originally published by Middleton [34]. This type of map is based on U, Th, and K airborne-radiometric maps released by Geoscience Australia [10,22]. Essentially, these data represent an approximation of the surface heat generation for all the rocks in each map pixel, which has dimensions of approximately 1.3 × 1.3 km of variable rock outcrop. However, such an average may not be representative of any particular outcrop that may fall in the approximate pixel area of 1.3 × 1.3 km. Accordingly, while such maps are a good general guide to high heat generation regions, the actual heat generation values may be several times less than specific geological units. As shown in Figure 6, the Darling Range has a surface radiometric heat generation in the range of 2.5–5.0 $\mu W\ m^{-3}$, which is lower than the field measurement of all the outcropping granites in the region. This, however, might be expected, as the data in Figure 6 represent an average of outcropping rocks in the pixel area of 1.3 × 1.3 km. Nevertheless, the map may provide a good general guide to regions of high surface radiogenic heat generation.

Very little is known about spatial variation of heat generation (and indeed U and Th concentration) in radiogenic granitoids in the Darling Range of Western Australia. Table 2 of Middleton [16], and included in Table 1 of this work, cites the variation between four sites at the Glen Forrest (J Forrest Pk 1–4 in Table 1) location. These four sites were within a total distance of about 100 m, and are within and around an abandoned granite quarry. The purpose

http://dx.doi.org/10.5772/61963

of these closely spaced measurements was to investigate the spatial variability of heat generation over small distances within a batholith. The table indicates that local heat generation within this batholith can vary between 6 and 8 μW m^{-3} over the 100 m. These observations suggest that heat generation within the batholith is relatively constant over such distances. The study of Jaeger [4] also found fairly constant heat generation values (mean of 8.9 μW m^{-3} with a standard error of 0.6 μW m^{-3}) over a borehole depth interval of 300 m within a radiogenic granite near the town of Doodlakine, located also in the Yilgarn Craton (see Figure 1) Jaeger's measurements lie about 1 km to the east of where the present measurements were made (see Table 1, 8.2 μW m^{-3}). Also, a study of several surface sites within a hot granitoid body in the Dunsborough region of the Southern Perth Basin (Table 1) exhibits a range of heat generation (12.3–15.7 μW m^{-3}, based on U, Th, and K concentrations) within an approximately 500-m stretch of land, which is assumed to comprise the same granitoid body. Spatial variability of U, Th, and A_0 within single granitoid bodies is a subject that requires considerably further work.

Heat flow at the base of granite batholiths (Q_b) in the Yilgarn Craton and Perth Basin is poorly known. Conclusions that can be drawn from the work of Jaeger (1970) are that (1) heat flow at the base of his presumed Yilgarn upper-crustal heat-generation layer is about 0.63 heat flow units (hfu, which convert to 26.4 mW m^{-2}) and (2) the radiogenic upper-crustal layer is about 4.5 km thick. Later works [34,35] in the central Perth Basin indicate that it commonly possesses a heat flow in the vicinity of 86 mW m^{-2}. However, in a locality at the Gillingarra 6 water bore (G6 in Figure 16), surface heat flow was found to be approximately 130 mW m^{-2} [34], which is anomalously high for the central Perth Basin. One could conclude that this thermal anomaly is due to anomalously elevated heat generation in the granitoids underlying the G 6 locality. On the basis of the results from the anomalous G 6 data, a range for the radiogenic heat generation from granitoids under the Perth Basin may be proposed from a simplification of Eq. (1), which is $Q_s = Q_b + A_1H_1$. Thus, in the non-anomalous situation, if Q_s = 86 mW m^{-2}, Q_b = 26 mW m^{-2}, and H_1 = 5 km, then the radiogenic heat production in the sub-basin granitoid layer is estimated to be 17.2 μW m^{-3}. However, in the anomalous case at G 6, if Q_s = 130 mW m^{-2}, Q_b = 26 mW m^{-2}, and H_1 = 5 km, then the radiogenic heat production in the sub-basin granitoid layer is estimated to be 26 μW m^{-3}. Both of these values (17.2 and 26 μW m^{-3}) for heat generation appear to be unreasonably high. Perhaps, as suggested by Middleton [34,41], the G 6 temperature anomaly may be caused by either anomalous thermal conductivity or convective groundwater flow. This currently remains unresolved. These observations are consistent with other regional studies [41].

For temperature modeling, it is important to establish mean annual surface temperature data that are necessary to estimate geothermal gradients [7,16,35]. These data can be derived from Australian Bureau of Metrology data covering the past five or six decades in the Perth Basin and other Western Australian basins. The difficulty is to how to process these data to arrive at a meaningful mean surface temperature that is relevant to geothermal processes. This is beyond the scope of this paper. For the purposes of modeling in the current study, a value for T_s of 21 °C is assumed, which is consistent with values proposed by Jaeger [4].

Temperature modeling for the Darling Range granitoids [16], and Table 3, was carried out using the geometry shown in Figure 3 and based upon Eq. (3). The purpose of the modeling is to determine if temperatures in the metropolitan Darling Range are high enough to support geothermal applications. In this modeling, the assumed parameters are the thicknesses of the radiogenic granite batholith (L) varying between 3 and 6 km. The complete temperature profile from surface (z=0) to a maximum depth of 4 km (N.B. to only 3 km in the 3-km-thick batholith case) has been modeled. The temperature versus depth for uniform heat generation of 4, 6, 8, 10, and 12 μW m^{-3} within the granitoids is calculated for batholith thicknesses of 3, 4.5, and 6 km. The results are shown in Figure 14 with L= 3 km (Figure 14a), L= 4.5 km (Figure 14b) and L= 6 km (Figure 14c). The thermal conductivity is assumed to be uniform at 3 W m^{-1} °C^{-1} [36]. The red curve also shown in Figure 14 represents the temperature versus depth in the absence of the radiogenic granite layer. The temperature in this case is estimated from a constant background heat flow of 24 mW m^{-2} (geothermal gradient of 8 ºC km^{-1}). In all cases, the temperature gradient is less in the absence of the radiogenic granite. The modeling suggests that a maximum temperature of approximately 100 °C may occur at 3000 m within a granitoid body with depth extent of 6 km that possesses a uniform heat generation of 12 μW m^{-3}. Certainly, such bodies have been observed from surface measurements, but the complete geometry and petrophysical makeup of these bodies are poorly understood.

PARAMETER	VALUE						
	CASE 1	CASE 2	CASE 3	CASE 4	CASE 5	CASE 6	CASE 7
A_o (μWm^{-3})	4	10	20	4	10	20	8
K (Wm^{-1}K^{-1})	3	3	3	3	3	3	3
L (km)	2	2	2	6	6	6	3.5
Q_b (mWm-2)	26.3	26.3	26.3	26.3	26.3	26.3	26.3
T_s (°C)	20	20	20	20	20	20	20

Table 3. Parameters assumed for the temperature modeling for the Darling Range region for the seven cases investigated, wherein the temperature profile versus depth is shown in Figure 13.

Perhaps a more realistic situation may entail a granitoid of depth extent of 4.5 km (which is consistent with Jaeger [4] and uniform heat generation of 8 mW m^{-2}). In this case, one is looking at almost 50 ºC at about 2000 m. Although this scenario cannot be used for most air conditioning and electricity uses, it is viable for recreational activities. It should be finally noted that this modeling is applicable only for the Darling Range vicinity of the Perth metropolitan area, which essentially comprises granitoid or latertic–granitoid-derived rocks. The Perth metropolitan area to the west of the Darling Range comprises over 15 km of Paleozoic sediments. It is presumed that the underlying rocks are similar to the Darling Range. This has yet to be conclusively confirmed.

http://dx.doi.org/10.5772/61963

3.2.2. Perth metropolitan area

The concept of recovering geothermal energy from the Yilgarn Craton is significantly enhanced by the presence of the city of Perth, the capital city of Western Australia, located near the western margin of the craton. The Darling Range is a physiographic expression of the Yilgarn Craton on the eastern edge of the Perth metropolitan area. Before 2010, only a few values of heat generation were available in the literature for the Yilgarn Craton [4,16]. However, studies have been carried out by the Western Australian Geothermal Centre of Excellence (WAGCoE) from 2009 to 2013 [42]. This centre carried out extensive studies on the potential of geothermal energy in Western Australia, and perhaps culminated in the concept of the "geothermal city" by Regenauer-Lieb et al. [43] and geothermal modeling of the Perth Basin by Schilling et al. [44].

The interest in geothermal energy was initially directed toward electricity generation. However, Ballesteros [45] noted that there had been steady growth in the direct use of geothermal heat in Western Australia, especially in the Perth metropolitan area. He reported that 12 sites were using, or were in development, geothermal heat for community or industrial projects. Pujol et al. [46] and Ricard and Pujol [47] have reviewed the previous 20 years of exploitation of the Yarragadee aquifer in the Perth Basin for direct-use geothermal heat. These authors have indicated how the face of geothermal energy in Western Australia has changed from a perception of electricity creation to direct heat energy extraction.

3.3. Northern Perth basin

The northern Perth Basin is bounded by the Northampton Complex to the north and the Yilgarn Craton to the east. Reasonable U and Th data are known from the Northampton Complex and airborne data are available for the Yilgarn Craton to the east. The Northampton Complex (see Figure 1 for location), which is part of the Pinjarra Orogen, has been mapped on the Geological Survey of Western Australia's Geraldton and Ajana 1:250,000 geological sheets [48]. The Northampton Complex forms the pre-sedimentary "basement" of the northern part of the Perth Basin, which is considered to possess appreciable geothermal energy potential, due to high temperatures observed within the sediments of the adjacent basin [12,50]. The high temperatures are presumed to be caused by elevated heat generation in the underlying Northampton Complex rocks.

Little recent geological work has been carried on the Northampton Complex. The Northampton Complex (see Figures 1 and 2 for location) has been mapped on the Geraldton and Ajana 1:250,000 geological map sheets [48], and is part of the larger Pinjarra Orogen, which lies along the western margin of onshore Western Australia. On the Ajana 1:250,000 geological sheet, the Northampton Complex is dominated by rocks described as granulite and gneiss. These rocks have been metamorphosed under pressures in the range of 600–900 MPa (6–9 kBar) and temperatures in the range of 600– 800 °C (upper amphibolite-to-granulite facies metamorphic conditions; Sanders and McGuiness [50]). These rocks are not dissimilar to those of the Leeuwin Complex, which is also considered to be part of the Pinjarra Orogen. The merged thorium aero-radiometric map (Figure 2) suggests much of the Northampton Complex region,

which consists of rocks with greater than 19.5 ppm thorium, noting that the proposed upper cutoff for the aero-radiometric maps for thorium is 19.5 ppm, as discussed above. However, also mentioned above and evident from ground-based studies in the Leeuwin Complex and Darling Range, one should be aware that 19.5 ppm appears to be the limit on the calibration technique of aero-radiometric observations for thorium, rather than a peak value that might be observed at the earth's surface. Laboratory-based values of concentration reported by Sanders and McGuiness [50] suggest that some localities may be significantly higher (i.e., > 39 ppm) than the aero-radiometric threshold maximum of 19.5 ppm.

Sanders and McGuiness [50] reviewed the geochemistry of the Ajana 1:250,000 geological sheet, and therein presented the valuable data concerning the surface distribution of thorium in the regolith. For the purposes of this study, the regolith is defined as unconsolidated or indurated weathered rock, and includes residual and transported material that can cover and obscure the underlying bedrock. The thorium concentrations reported in this review are from the Geological Survey of Western Australia map of Sanders and McGuiness [50], and the values were measured by the recognized laboratory methods referenced in the Sanders and McGuiness' study. Their map is reproduced as Figure 15 in this chapter. The study presented a systematic grid of surface thorium concentrations in outcropping rocks at a spacing of approximately 5–10 km, nominally one sample per 16 km^2. The map of Sanders and McGuiness displays a range of thorium concentration between approximately 5 and > 39 ppm. Unfortunately, the upper limit of thorium concentration in the study, although acknowledged to be greater than 39 ppm, is not reported in their report.

Rocks from the Northampton Complex are very likely to extend under the north Perth Basin, and they probably contribute to the high temperatures observed in petroleum wells in that region [12,35]. Little definitive work has been carried out to date on the influence of radiogenic elements in the basement rocks upon elevated temperatures in the sediments of the north Perth Basin. Basement rocks have also been intersected in a number of petroleum wells. Table 4 shows an analysis of the gamma-ray log response found in the basement rocks in this part of the basin. The table also shows the gamma-ray log response for high-organic shale formations and some sandstones in the observation well for comparison with the basement rocks. Equation 8 is used to convert gamma-ray (GR) data from the wells to heat generation (A_0) data. Heat generation in basement rocks determined by this method is seen to be in the range of 2.0–5.6 μWm^{-3}.

Thorium values mapped on the Ajana 1:250,000 geological sheet from Sanders and McGuiness [50] reflect relative heat generation as expressed in Eq. (4). Surprisingly, high Th is also found in the sedimentary rocks on the margin of the northern Perth Basin, but it does not appear to be especially dominant in the surrounding igneous and metamorphic rocks. The provenance of high radiogenic elements in sediments of the northern Perth Basin (perhaps also the southern Carnarvon Basin) is currently an imponderable. Further studies are needed to fully understand the geology, geochemistry, and geophysics of the northern Perth Basin and Northampton districts.

http://dx.doi.org/10.5772/61963

Well Name	Basement Depth (m)	Structural Location	GR av. (API)	GR max. (API)	Range of Heat Generation, Ao (μWm^{-3})	Reference lithology GR av. (API units)
Arramall 1	2225		280	280	**4.5**	260, PCS
Arrowsmith 1	3420		180	230	**2.9 – 3.7**	120, HS; 100, K
Bookara 1	852		150	195	**2.4 – 3.1**	135, K
Bookara 3	1560		168	204	**2.7 – 3.3**	144, K
Sue 1	3054		255	265	**4.1 – 4.2**	270, PCS; 140, V
Conder 1 hot sandst.	203-213		> 400	> 400	**> 6.4**	140, K
Conder 1 basement	229		180	230	**2.9 – 3.7**	140 K
Jurien 1	3280		140	165	**2.2 – 2.6**	150, PCS
Wendy 1	1211		220	280	**3.5 – 4.5**	40, TS
Cadda 1	2743		125	200	**2.0 – 3.2**	150, PCS
Woolmulla 1	2804		50	160	**0.8 – 2.6**	70, PCS
Beharra 1	2075		155	162	**2.5 – 2.6**	140 PCS
Drakea 1	3048		225	255	**3.6 – 4.1**	195, K;
Cliff Head 1	1480		170	195	**2.7 – 3.1**	180, PCS
Connolly 1	450		195	218	**3.1 – 3.5**	180, K; 200, PCS
Wattle Grove 1	799		260	350	**4.2 – 5.6**	150 K
Mountain Bridge 1	3385		250	? 350	**4.0 - ? 5.6**	150 K
North Yardarino 1	2190		-	-	**-**	NPD
Woodada 19	2035		-	-	**-**	NPD
Dunnart 1	?		?	?	**?**	Dubious data
Hovea 2	?		?	?	**?**	Data accessibility ?
Dongara 6	1540		-	-	**-**	NPD

Reference lithology code for Table 4. HS: Holmwood Shale (Permian); PCS: Permian coals and shale; IRCM: Irwin River Coal Measures; V: Volcanic intrusives (? Cretaceous); K: Kockatea Shale (Triassic); TS: Tumblagooda Sandstone; NCR: No Petrophysical Data (for gamma-ray). See Mory and Iasky (1996) for reference to stratigraphic units.

Table 4. Northern Perth Basin with U, Th, K & A_o derived from petroleum well data. The figure shows showing gamma-ray log (GR) responses from basement rocks with established crystalline basement intersections and derived sediments. Reference gamma-ray units (API) within the overlying formations for various wells in the Perth Basin are shown for confidence in gamma-ray logging in API units. The heat generation calculation, derived from observed log-derived GR data is $A_o = 0.015$ (GR) (see text for explanation).

4. Pilbara region

The Pilbara region of Western Australia contains some of the state's most significant mineral deposits. However, difficulties can arise for the development of these mineral resources due to the remoteness and lack of economic energy supply. The energy supply for mines at remote locations in this region is commonly sourced by diesel-powered generators, although some mines are supplied with gas from the North West Shelf. Geothermal energy may provide an economic alternative, or additional energy supply, if access to deep radiogenic granitoids is available. Hot Dry Rock geothermal systems are one of three ways that are considered viable for using geothermal energy in Australia. The three systems are (1) direct heat extraction, (2) Hot Sedimentary Aquifers (HSA) energy conversion, and (3) the Hot Dry Rock geothermal regime [12,51]. The HSA system, as well as direct heat extraction, is currently being explored by a number of companies as a possible system for both power generation and air conditioning in Western Australia. An HDR system is being exploited in the Cooper Basin by the geothermal company Geodynamics Limited. The HDR system entails injecting cool water into hot fractured rocks at depths of about 4 km, allowing the water to percolate through the hot rocks (which heats the water), and then extracting the hot water for geothermal energy applications. Geothermal explorers commonly seek temperatures in excess of 200 ºC for such systems. The hot water is fed into various types of turbines for electricity generation; the efficiency of electricity generation is dependent on the temperature of the fluid being introduced into the turbine.

Two regions of high radiogenic heat generation can be seen in Figure 2. The two hot regions are identified to be within the Numbana and Coolegong mesogranite intrusions. These intrusions are late-stage, highly fractionated granites [52,53] known to possess high U and Th concentrations, which crop out at the surface. Table 1 shows U and Th versus radiogenic heat generation (A_0) of samples of the Numbana and Coolegong granites (data courtesy of the Geological Survey of Western Australia). An excellent linear trend has been found between U and heat generation (A_0). The linear regression curve through U and A_0 data from Pilbara and Yilgarn Craton granitoids exhibit a simple relationship [16]:

$$U = 2.2A_0 - 5.4, \tag{9}$$

where U is the uranium concentration (ppm) and A_0 is the radiogenic heat generation (μWm^{-3}); the coefficient of linear regression (R^2) is 0.92. As mentioned previously, the U and Th (essentially reflecting heat generation) of the rock samples are generally higher than the values observed from the airborne data [16]. These data suggest that the radiogenic heat generation in the mesogranites of the Pilbara Craton may be as high as 13 μWm^{-3}, which is in the vicinity of those observed in the Leeuwin Complex in south west part of Western Australia.

Figure 18 shows temperature models displaying expected temperature versus depth within the two granitoids in the Pilbara region. The numbers on each curve represent the thickness (in km) of a granitoid with a uniform heat generation of 12 $\mu W\ m^{-3}$. Temperatures at depths

http://dx.doi.org/10.5772/61963

within the granitoids of 3–4 km may be over 100 ºC, but these require drilling with large-diameter bore holes to those depths through crystalline rocks. Currently, this does not present an economic development.

New generations of turbines, for example, Kalina cycle and variable phase turbines [54,55], are allowing the use of lower-temperature geofluids for electricity generation. A stand-alone variable phase turbine has been designed to generate about 1 MW of electricity with input fluid temperatures of about 110 ºC, although greater generation efficiencies are obtained at higher temperatures. These new generation of turbines may hold significant implications for generating power at Pilbara mining sites. The key ingredient is the proximity of a hot granite to a mine location. Figure 2 shows the approximate radiogenic heat generation of surface rocks on the Marble Bar 1:250,000 map sheet. The map is generated from calibrated uranium, thorium, and potassium elemental abundances determined from airborne radiometric surveys [9,34]. The U, Th, and K abundances are converted to approximate radiogenic heat generation by a method described by Kappelmeyer and Haenel [23].

5. Carnarvon and Canning basins

Apart from Perth Basin, HAS geothermal resources have been shown potentially to exist in the Carnarvon and Canning basins [12,51]. Some further work has been carried out for this review on the Carnarvon Basin, which explores, in a preliminary sense, the anomalous elevated temperature regime in the southern Carnarvon Basin. For the Canning Basin (Figure 1), little new geothermal insight has been gained since the study of Hot Dry Rocks [57], which was commissioned by the Geological Survey of Western Australia. Beardsmore and Cull [7] have reported some important heat generation data derived from gamma-ray logs in that basin. Their approach has been used earlier in this chapter to attempt to understand heat generation and the presence of radiogenic elements. Given the lack of new data from the Canning Basin, only the Carnarvon Basin will be discussed further.

5.1. Carnarvon basin

High temperatures have been recognized in the Southern Carnarvon Basin (Figure 1). These elevated temperatures have been reported in various studies [12,51,56]. This region is probably the most prospective region in Western Australia for geothermal energy, behind the Vasse Shelf region in the southern Perth Basin. However, very little geothermal exploration has been carried out in the region. However, substantial evidence supports the premise that the Carnarvon Basin may be able to supply the Pilbara mining communities with not only (1) long-term geothermal-sourced electricity (looking beyond North West Shelf-sourced gas supply, i.e., beyond perhaps 2050), but also (2) intermediate-term nearby resource projects and tourism enterprises. It is of note that Davidson [58,59] described the Peninsular Hot Spring tourist enterprise in southern Victoria, which entertains an estimated $75 million per annum regional economic benefit. Such enterprises are potentially available to environmentally sensitive, but tourist intensive, coastal resort sites from Carnarvon north to Exmouth.

5.1.1. Geology and geophysics

The geology of the southern Carnarvon Basin is well understood, having been described by Hocking et al. [60], Hocking [61], and the geothermal potential by Ghori [12]. The geology of the North West Cape, which is especially relevant to the current article, was studied by Malcolm et al. [62]. It has been shown from petroleum drilling data that an unusually hot region exists along the coastal region from Shark Bay to the Exmouth Peninsula, and maybe for some distance inland toward, and perhaps including, the outcropping Pilbara Craton. It is reasonable to expect that the Pilbara Craton underlies a reasonable amount of the onshore Carnarvon Basin between Shark Bay and Exmouth, including the North West Cape. Further, it is expected that the Pilbara Craton may contain some radiogenic granitoids in this region. There appears to be no detailed scientific study of why the elevated heat flow occurs in this region, despite it being covered since 2010 by seven GEPs. According to the studies by Ghori [12,51], temperatures in excess of 150 ºC may exist between drillable depths of 3000–4000 m, and these wells have a geothermal gradient in the range of 60–100 ºC/km (figure 2 from Ghori [12]).

5.1.2. A geothermal puzzle

The unanswered geothermal puzzle of the southern Carnarvon Basin is centered on the cause of the elevated geothermal gradients in the Exmouth and Gascoyne subbasins. Essentially, the puzzle may condense into whether the elevated temperatures reported by Ghori [12,51] are caused by underlying radiogenic granitoids or by the flow of deep hot groundwater into surface sediments. No extensive studies have been carried out to understand this phenomenon. The source of the observed high heat flow in petroleum wells appears to be generated from high radiogenic granitoids that underlie the deep sedimentary blanket in the region. However, this is only a circumstantial evidence, and without sufficient further investigation, it cannot be stated with certainty. Convective heat transport should not be ruled out as the cause of these elevated temperatures. Comparison to the surface geological units to elsewhere in Western Australia suggests that the sedimentary cover may have a surface heat generation in the vicinity of 1 μWm^{-3} (see Table 4, and Beardsmore and Cull [7]). On the adjacent Pilbara Craton, outcropping granitoids possess heat generation values of up to 5 μWm^{-3} in the adjacent Pilbara Craton; these may translate up to 12 μWm^{-3} in specific geologic units on the ground. Therefore, the granitoids that are interpreted to underlie the Carnarvon Basin in the cross section in Figure 19 may possess a heat generation of up to 12 μWm^{-3} or more. This heat generation value is typical of radiogenic granitoids underlying the Perth Basin, and also the central Australian Cooper Basin [6], where geothermal energy is currently being developed. The WAPET Cape Range petroleum exploration wells are known to encounter bottom-hole temperatures in excess of 140–160 ºC at depths between 4300 and 4600 m; these temperatures are probably greater after fluid stabilization in the drill hole. Figure 19 shows that the total sedimentary blanket over interpreted high heat-generating granites may be up to 9 km [61,62].

5.1.3. Temperature modeling

Based on the cross section [56] shown in Figure 19, several numerical models of the temperature versus depth for various heat-generation scenarios are shown in Table 5a. These are based on

http://dx.doi.org/10.5772/61963

the previously described 1D models for such situations as described in Eqs (1) and (2). The assumptions used to generate Table 5a are shown in Table 5b, and they are based on the surface radiogenic heat data derived from Figure 2 and Eq. (4), and also studies reported elsewhere in the literature [4,5,16,61]. Ghori [12] has shown from petroleum wells that the temperature gradient in the southern Carnarvon Basin can range between 30 and 100 ºC/km, and these are consistent with the temperatures generated in the models in Table 1. If convection is not involved, then the governing factor appears to be the heat generation of underlying granites. However, a disturbing observation from hydrogeological studies is that there are significant indications of hot artesian water movement in this basin. The static models in Table 5a demonstrate that temperatures at depths greater than 3000 m may have temperatures significantly greater than 200 ºC, depending on the heat generation of underlying granite bodies. In the upper side of the models, one is looking at full steam-type turbines for the generation of electricity, which are the current optimal geothermal energy-producing technology, and is common place in New Zealand, Indonesia, and California. A caveat needs to be placed on the geothermal activity in this basin centered around the balance of radiogenic heat input versus convective heat input. More investigation is required.

Heat Generation ($\mu W\ m^{-3}$)	**Geothermal Gradient (°C km^{-1})**	**Temp @ 2 km (°C)**	**Temp @ 3 km (°C)**	**Temp @ 4 km (°C)**
3	42	104	146	188
6	60	140	200	260
9	78	176	256	332
12	96	212	308	404

(a)

PARAMETER	**VALUE (units)**	**COMMENT**
Sediment thickness	4000 (m)	Varies between 2 and 8 km
"Hot" granitoid thickness	6000 (m)	May vary between 2 and 8 km
Basal heat flow	24 (μWm^{-3})	Assumed from Perth Basin
Surface temperature	20 (°C)	Can be higher
Thermal conductivity	3 ($Wm^{-1}°C^{-1}$)	Variable between 2 and 5 units

(b)

Table 5. Carnarvon Basin modeling results (a) temperatures and (b) assumptions. See also the geological cross-section in Figure 19 for geological consideration discussed in the text.

6. Time-variant considerations

It may be worth examining some time-variant models for heat flow and temperature variation for Western Australian geothermal scenarios. These are largely based on applications of Eq.

(3) [24], which considers the case where a layer of rock with high heat generation is rapidly placed at the earth's surface at a time $t = 0$. A typical situation for Western Australia may occur where lateritic enrichment occurs in the Tertiary Period. The question being posed is: does this enrichment in U and Th alter the temperature profile in the vicinity of the chemical alteration process, and, if so, how great is the temperature disturbance and how long does it take to stabilize? An initial intuitive guess would be that stabilization occurs fairly rapidly and there is not much disturbance to the temperature or heat flow regime. A lateritic profile in the Darling Range may be up to several hundred meters thick [40], but generally less than 100 m. A weathering profile on the Leeuwin Complex may be of similar thickness [63]. The question posed revolves around the difference that occurs for a heat-generating profile of thickness between 50 and 300 m at the surface. We can use the Meelup Park enrichment value (Table 1) of 40 μW m^{-3} as an initial test.

Carslaw and Jaeger [24] propose that the surface geothermal gradient for a geometry shown in Figure 3, where a heat-generating layer (injection of fluids or erosional enrichment) occurs rapidly, can be described by an equation of the type:

$$\Delta Q_R = 2A_0(\alpha t)^{1/2}\left\{1/(\pi)^{1/2} - \text{ierfc}\left[L/(4\alpha t)^{1/2}\right]\right\}, \tag{10}$$

where ΔQ_R is the heat flow contribution of the radiogenic layer in units of mW m^{-2}, A_0 is the uniform heat generation in the layer in μW/m^3, α is the thermal diffusivity of the rocks in m^2s^{-1}, t is the time in seconds, L is the thickness of the radiogenic enrichment layer in m, and ierfc[x] is the integrated error function. This equation has been modified from the Carslaw and Jaeger [24] equation 6 by multiplication by thermal conductivity (K) to be expressed as heat flow rather than thermal gradient. Carslaw and Jaeger also indicate that this equation will reduce to the simple form of $\Delta Q_R = A_0 L$, where time becomes very large (> 10 million years) and L is less than 50 km. This was referred to earlier with regard to Eq. (1).

Some simple calculations with Eq. (9) indicate that stabilization of an enrichment layer, such as observed at Meelup Park (see Table 1 and Figure 9 for magnitude of Th anomaly) in the Leeuwin Complex and the Vasse Shelf, southern Perth Basin, will occur well within 1 million years of enrichment, where a 100 m of enrichment zone is assumed. A zone of 100 m may be expected, based on geological and environmental mapping [63]. Similar durations for thermal stabilization may also be expected for the lateritic zones in the Darling Range in the central Perth Basin, although such high levels of enrichment are not observed from current observations (see Table 1). These conclusions, based on numerical modeling, are consistent with expectations. In the case where $\Delta Q_R = A_0 L$, which is the stabilized case above, it is interesting to understand the influence that an enriched zone may have on heat flow. Table 6 shows a range of incremental heat flow (ΔQ_R) values that will occur for a range of heat generation (A_0) and enrichment layer thicknesses (L). The table indicates that enrichment zones may contribute an appreciable input to localized heat flow, especially if the thickness is greater than 100 m and heat generation is greater than 80 μW m^{-3}.

http://dx.doi.org/10.5772/61963

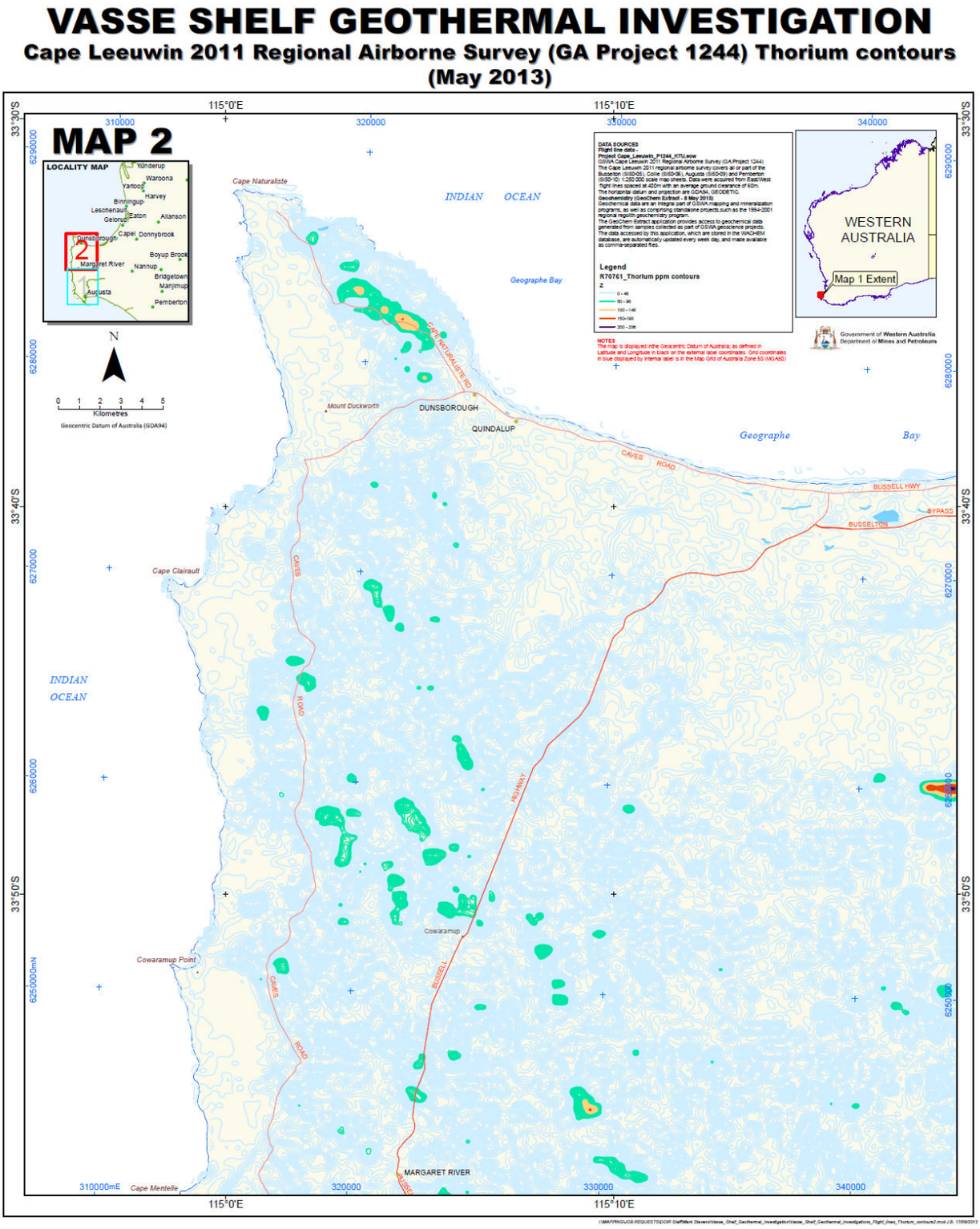

Figure 9. Thorium distribution in Dunsborough region (GSWA database).

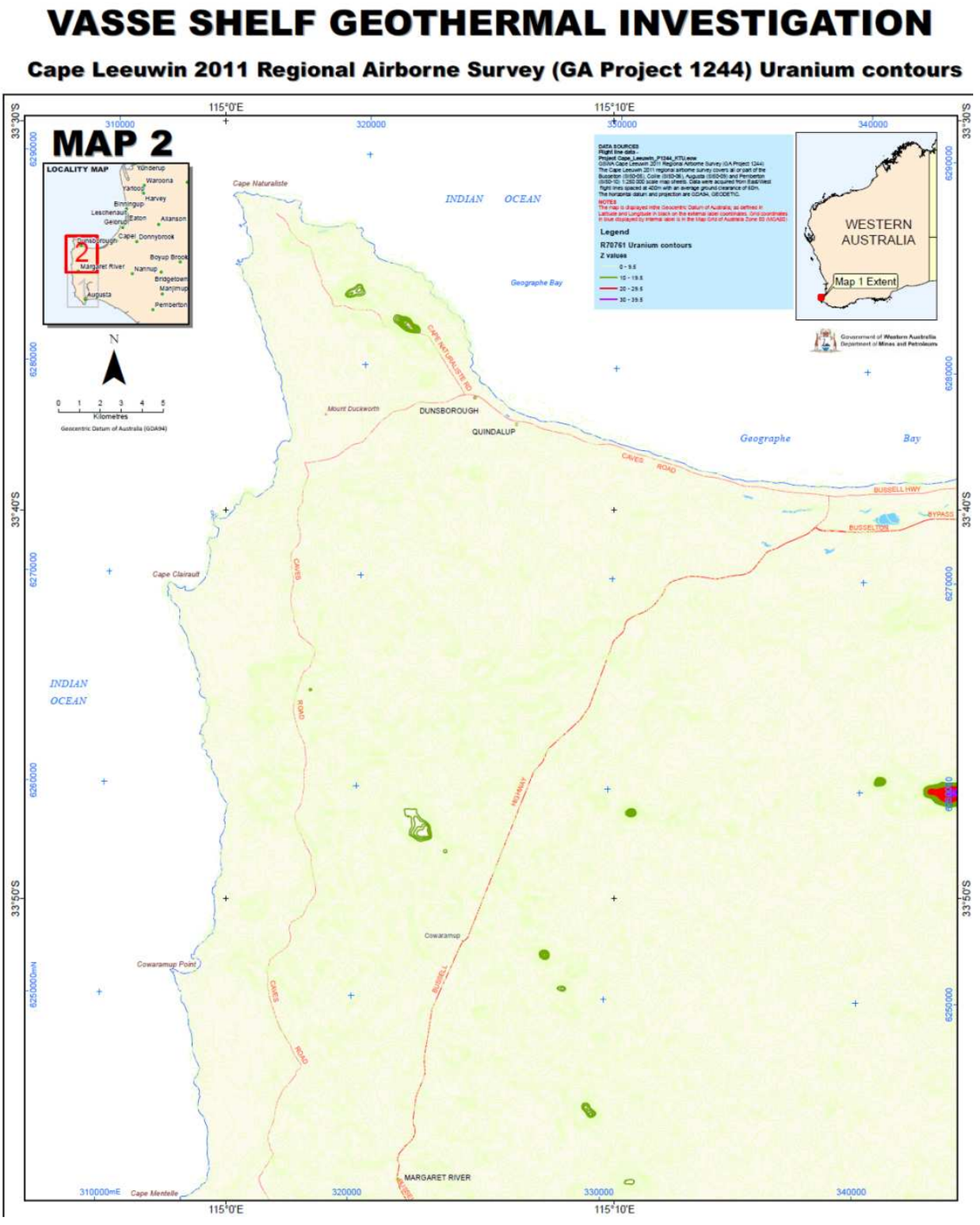

Figure 10. Uranium distribution in Dunsborough region (GSWA database).

http://dx.doi.org/10.5772/61963

L (m)	Ao (μW m^{-3})	ΔQ_R (mW m^{-2})
50	15	0.75
50	40	2.00
50	80	4.00
50	120	6.00
100	15	1.50
100	40	4.00
100	80	8.00
100	120	12.00
200	15	3.00
200	40	8.00
200	80	16.00
200	120	24.00
300	15	4.50
300	40	12.00
300	80	24.00
300	120	36.00

Table 6. Modeling results for shallow enrichment zones.

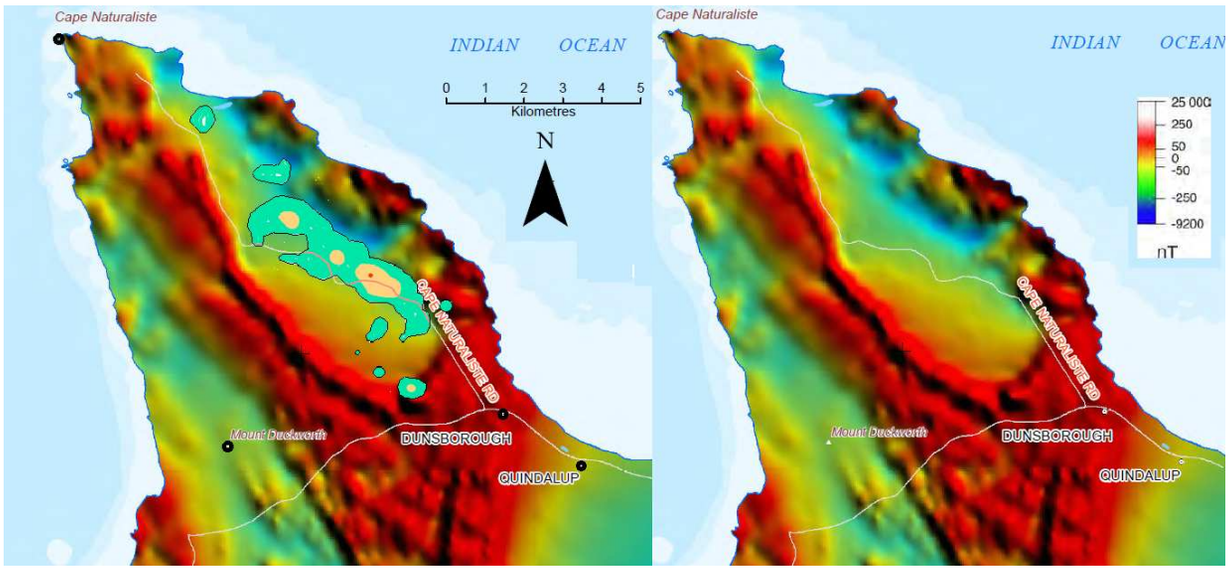

Figure 11. Magnetic anomalies and Th anomaly locations for the Leeuwin Complex and vase Shelf (south Perth Basin). The Th and associated heat generation anomalies appear to lie in magnetic medium to low areas. The map shows the aeromagnetics in the vicinity of Dunsborough with the location of the Th anomalies superimposed on the left-hand-side (LHS) image. The right-hand-side (RHS) image shows the aeromagnetics without the Th anomalies superimposed, and the color scale of magnetic intensity in units of nanotesla (nT). The magnitude of the Th anomalies (outline in black on LHS) is represented as green indicating 50–100 ppm, orange indicating 100–150 ppm, and red indicating 150–200 ppm. Ground measurements of Th indicate concentrations are in the order of 280 ppm in the orange regions.

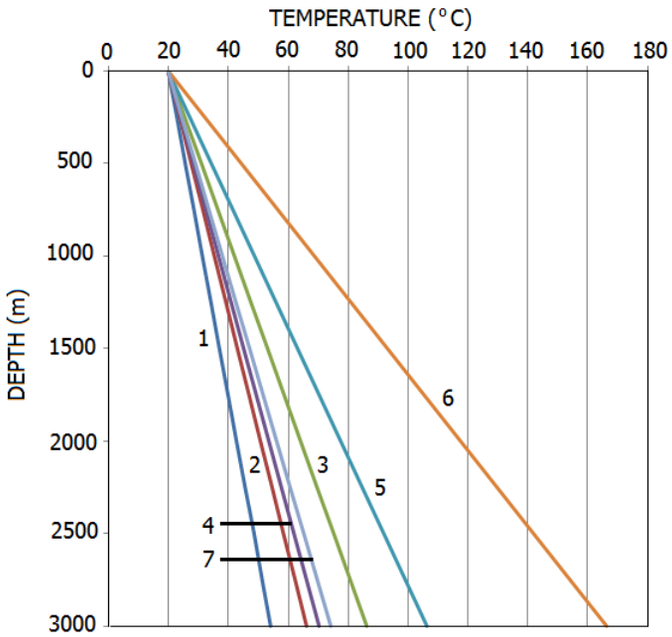

Figure 12. Temperature versus depth for the seven cases proposed in Table 2 for the south Perth Basin (Vasse Shelf). The number on each curve identifies the appropriate case in Table 2. The Wharton [37] study suggests that the temperature at 1000-m depth is approximately 40 °C. Cases 2, 3, 4, and 7 most closely satisfy this observation.

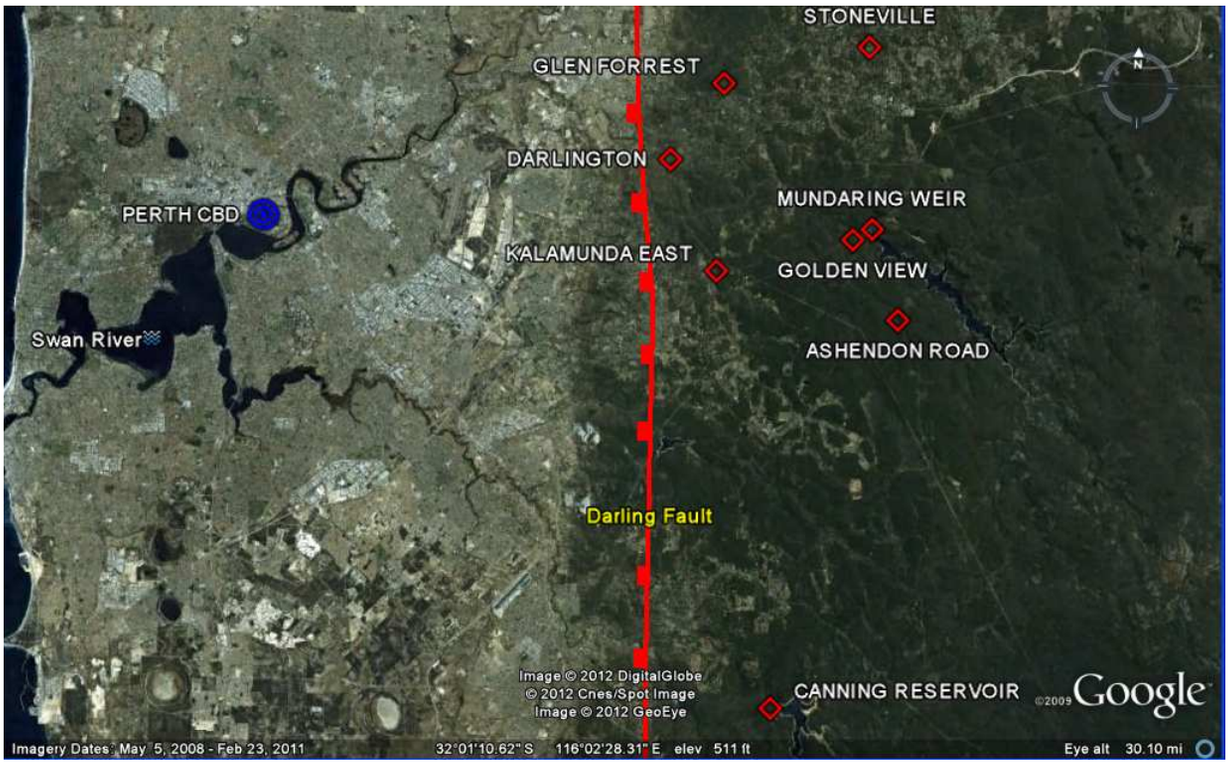

Figure 13. Image of the central Perth Basin (in the vicinity of the Perth metropolitan area and adjacent Darling Range): with some measurement localities (modified from Middleton [16]).

http://dx.doi.org/10.5772/61963

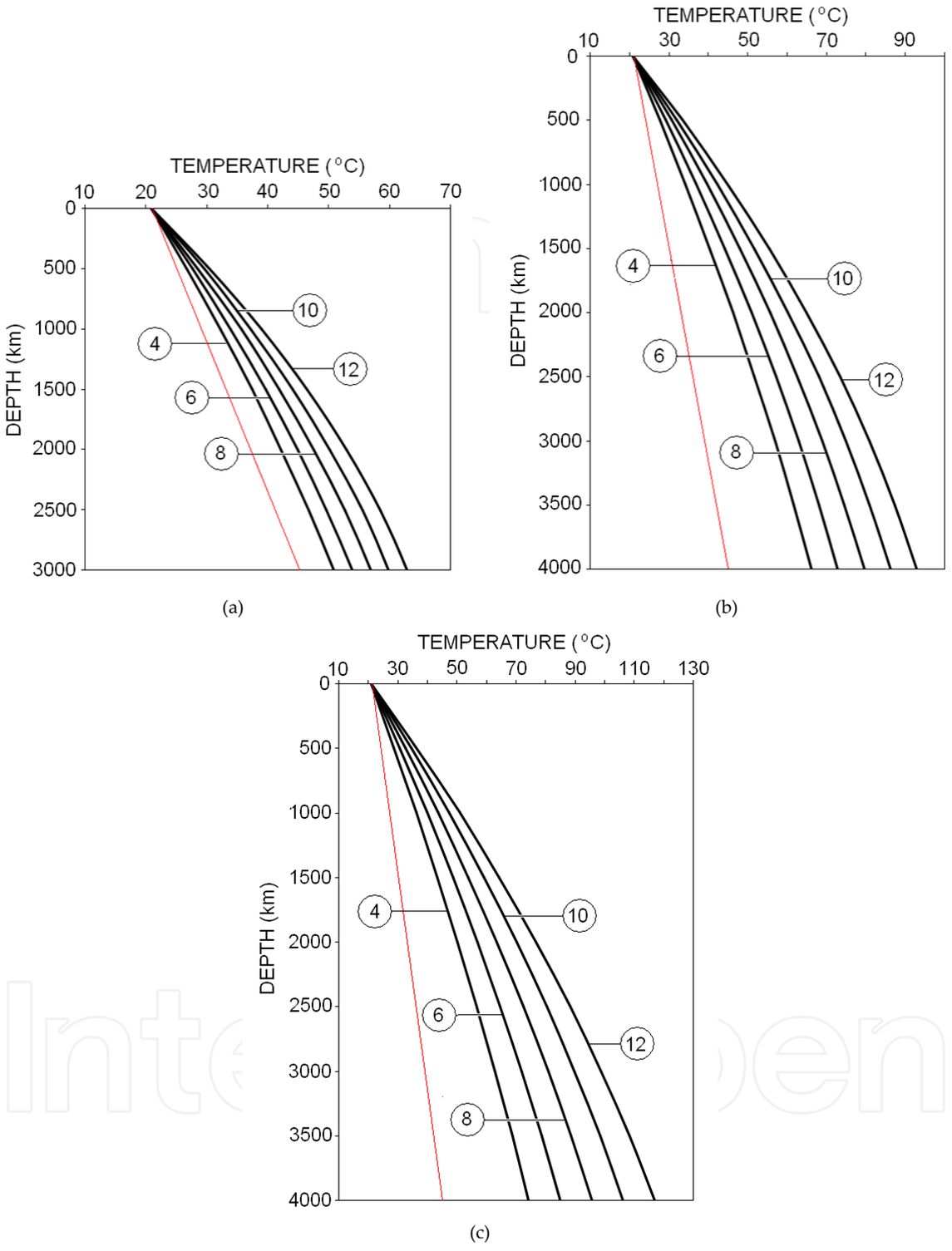

Figure 14. Temperature versus depth for the Darling Range [16]. The values shown in the circles are the assumed uniform heat generation in the radiogenic (granitoid) layer in units of μW m^{-3}. Figure 14(a) shows temperature versus depth with the radiogenic layer of depth extent of 3 km. Figure 14(b) shows temperature versus depth with the radiogenic layer of depth extent of 4.5 km. Figure 14(c) shows temperature versus depth with the radiogenic layer of depth extent of 6 km. The curves in red on 14a, 14b, and 14c represent the temperature versus depth profile, where there is no heat generation in the granitoid layer.

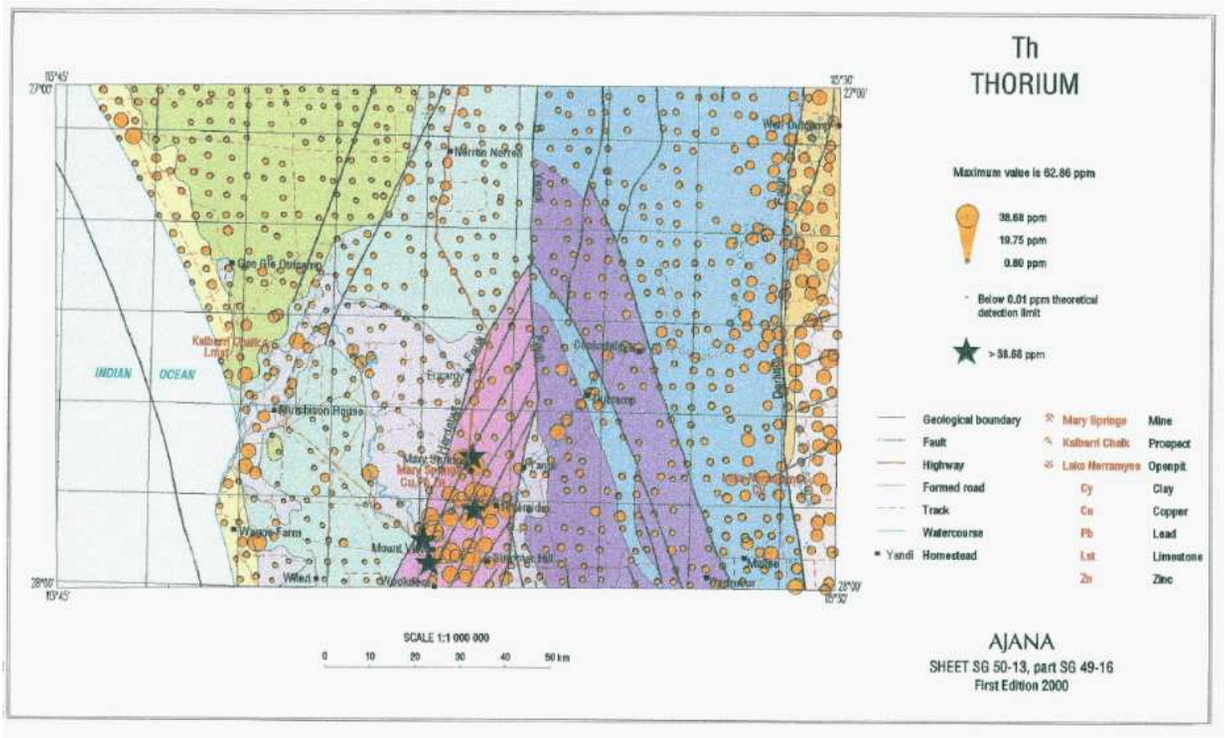

Figure 15. Thorium values Ajana 1:250,000 geological sheet from Sanders and McGuiness [50] are shown in this figure. The map also reflects the main contributing sources to heat generation in the vicinity of the northern Perth Basin and the rocks expected to underlie it. High Th is found in the sedimentary rocks on the margin of the northern Perth Basin, and it does not appear to be significantly less than the surrounding igneous and metamorphic rocks. The provenance of high radiogenic elements in sediments of the northern Perth Basin (perhaps also the southern Carnarvon Basin) is currently an imponderable. More work is definitely needed to understand the geology, geochemistry, and geophysics of the northern Perth Basin and Northampton district

http://dx.doi.org/10.5772/61963

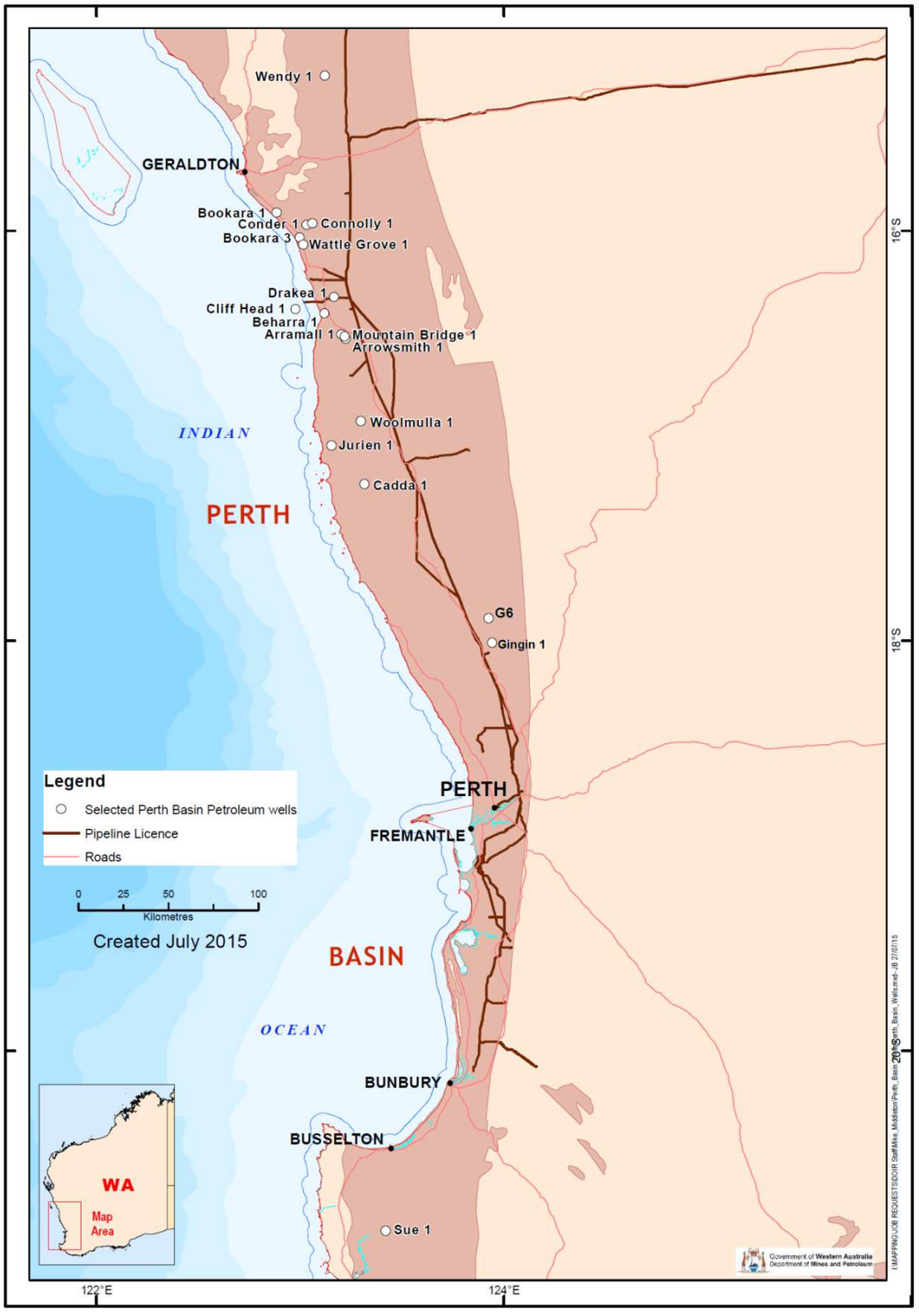

Figure 16. North Perth Basin well locations with basement intersections for potential heat generation estimations (combined with Table 4).

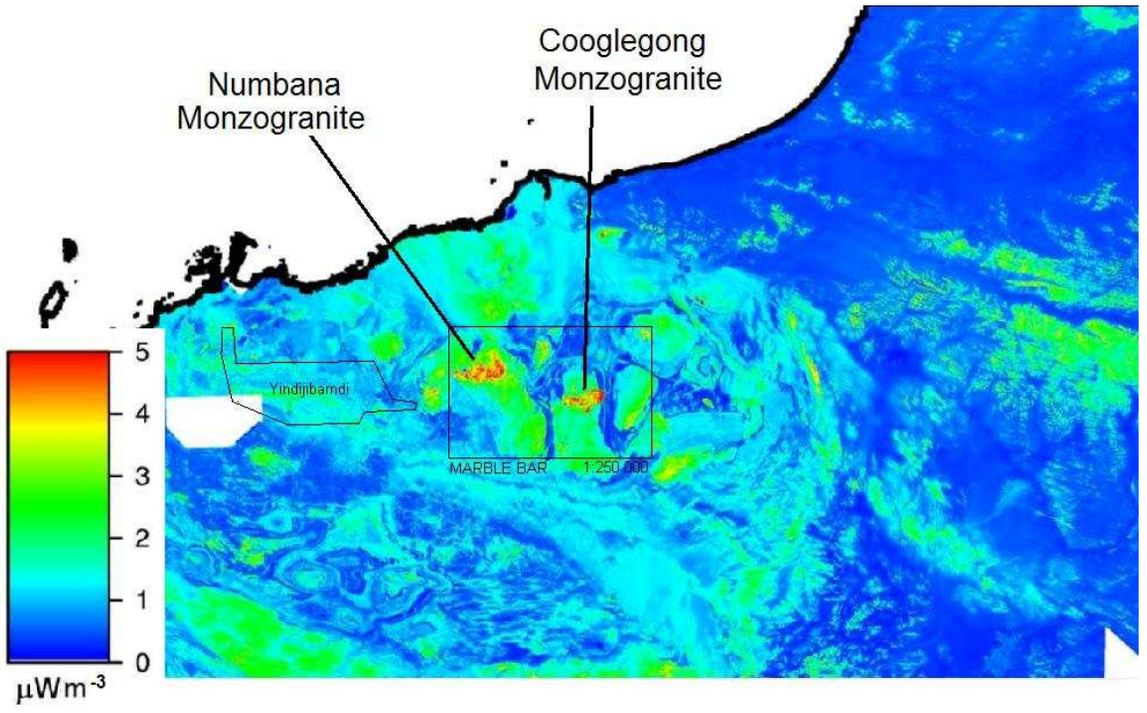

Figure 17. Pilbara Region hot granites. A map showing the integration of airborne U, Th, and K concentrations to reflect surface heat generation in the Pilbara region) [34]. The "hot" Numbana and Coolegong granitoid bodies are seen as the areas as shown in the image.

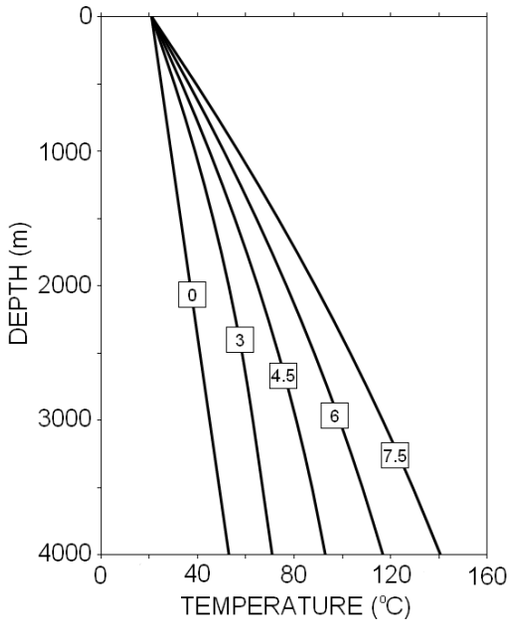

Figure 18. Pilbara temperatures for hot granites. The curves represent temperature versus depth for a radiogenic granitoid of uniform heat generation of 12 μW m^{-3}. The numbers on the curves represent the thickness of the radiogenic (granitoid) layer.

http://dx.doi.org/10.5772/61963

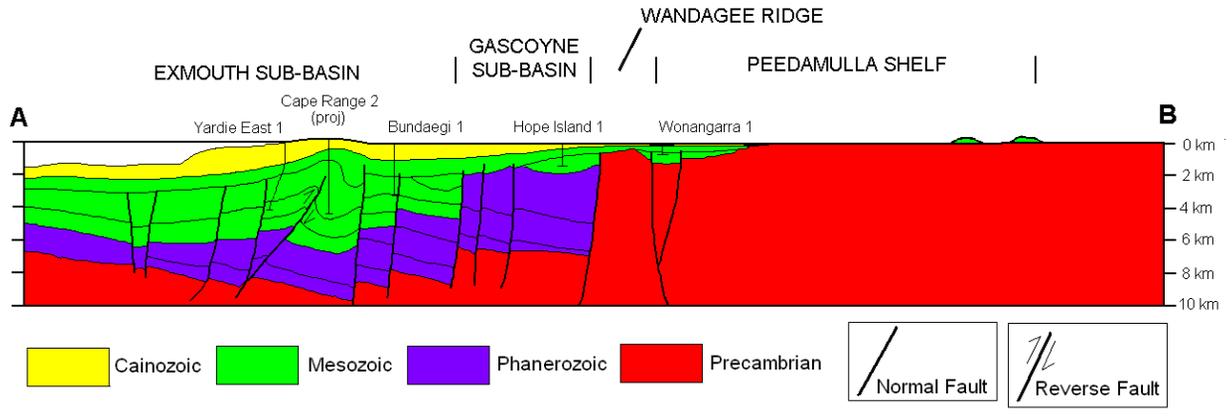

Figure 19. Carnarvon Basin summary (cross section). The red represents interpreted granitoid rocks that may possess radiogenic heat potential.

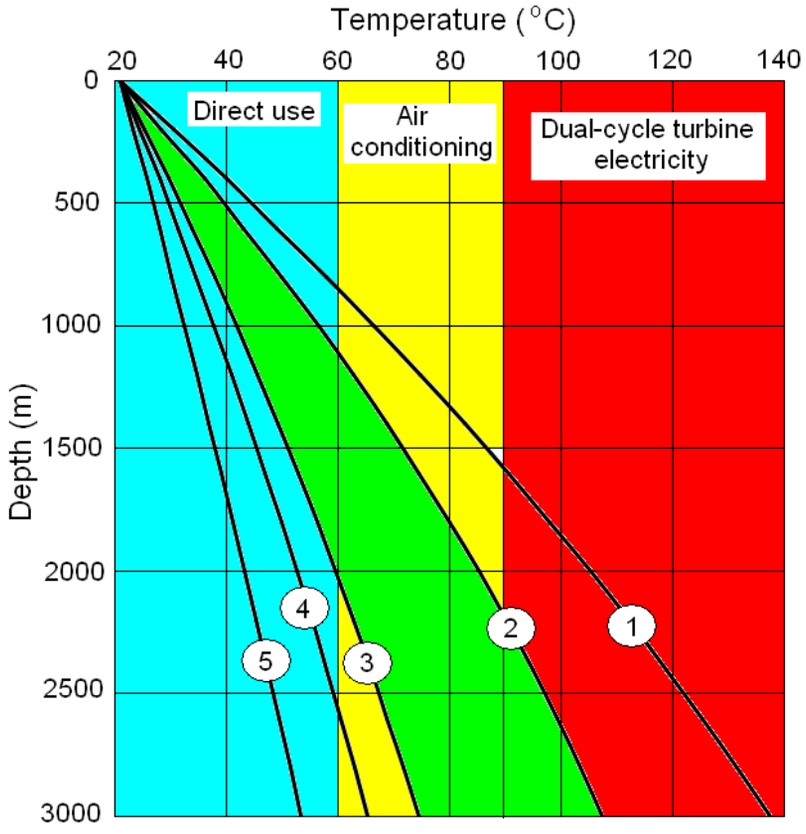

Figure 20. Figure showing known temperature regimes and possible geothermal energy development scenarios for Western Australia as of 2015.

7. Conclusion

In conclusion of this study, there are a number of generally low-temperature geothermal energy applications effectively operating in Western Australia [45–47]. The principal challenge for geothermal energy is to compete in the gas-rich economy of Western Australia. Figure 20 shows the current range of scenarios for temperatures versus depth in Western Australia. Case 1 is the current best case, where at about 2000 m, approximately 105 °C is encountered. It is anticipated that it can happen, but is not expected to be common on current geological and geophysical knowledge. Developments in the cases 3–5 are well known and are currently happening, and are common in the Perth metropolitan area. The green area in Figure 20 (between curves 2 and 3) is the space of current geothermal development, and regions in Western Australia that may take advantage of this temperature/depth range may be in the tourist areas of the southwest of Western Australia and the Carnarvon Basin-Cape Range regions. The transition to electricity (curve 5 and beyond) is challenging in the current economic climate, but may be anticipated to occur within the next 10–15 years.

The review recognizes that temperatures between 3000 and 4000 m in the Vasse Shelf may fall in the range of 90–150 °C. This temperature range is sufficient to permit electricity generation with organic Rankine cycle (ORC) or variable phase cycle (VPC) turbines [54,55], albeit with low efficiency. This temperature range is ideal for direct heat use for the tourist industry, for which the region is well known. Heat generation in radiogenic granitoids in the Darling Range is observed to fall in the range of 4–10 $\mu W\ m^{-3}$. The heat generation appears to be quite variable within the Darling Range region; however, there is some evidence that the heat generation may be fairly uniform within any particular batholith or location. In addition, there is a movement toward direct use for tourism and small-scale industrial usage. Significant geothermal projects are in the development stage for district air-conditioning, because Perth, which builds housing for a mild Mediterranean climate, experiences a wide temperature range from as low as 1 °C in winter to over 40 °C in summer. This reflects the direction of the current change in paradigm for geothermal in Western Australia.

Finally, in consideration of commercial geothermal energy production in the Western Australian region, the modeled temperatures cannot support current concepts of large-scale electricity generation with geothermal energy based on the *Hot-Dry-Rock-type* scenario, where it is generally accepted that temperatures are well in excess of 220 ºC.However, the new generation of low-temperature, organic-Rankine cycle turbines [54,55], and adsorption chillers, which operate in the vicinity of 100–150 ºC, could place the Vasse Shelf, Darling Range, and mining regions in the Pilbara in an advantageous economic position for alternative energy supply close to an existing market.

Acknowledgements

The technical help and advice of Mark K. Stevens, Ameed Ghori, Klaus Gessner, Lynn Reid, and Kerem Kanadarikrik from the Western Australian Department of Mines and Petroleum

http://dx.doi.org/10.5772/61963

is gratefully acknowledged for input into my geothermal studies over the past six years. The editorial skills of Karina Jonasson from the same organization have made a significant impact on the quality of the department's geothermal and other publications over these years. Encouragement from and discussions with, his friend and colleague, Mark Ballesteros, set the author on a unique direction within the geothermal path in 2009. This resulted in two extremely valuable symposia: Western Australian Geothermal Energy Symposium (WAGES) 2011 and (WAGES) 2012. Finally, the author wishes to acknowledge the Executive Director of the Petroleum Division in the Western Australian Department of Mines and Petroleum, Jeff Haworth, for permission to publish this work.

Author details

Mike F. Middleton*

Address all correspondence to: mike.middleton@dmp.wa.gov.au

Department of Mines and Petroleum, East Perth, WA, Australia

References

[1] Jacobs, J.A., Russell, R.D. and Tuzo Wilson, J., 1959, Physics and Geology, McGraw Hill Book Company Inc., 424p.

[2] Jeffreys, H., 1976, The Earth: Its Origin, History and Physical, Cambridge University Press, 612p.

[3] Lilley, F.E.M., Sloane, M.N. and Sass, J.H., 1978, A compilation of Australian heat flow measurements, *Journal of the Geological Society of Australia*, 24, 439–446.

[4] Jaeger, J.C., 1970, Heat flow and radioactivity in Australia, *Earth and Planetary Science Letters*, 8, 285–292.

[5] Sass, J.H., Jaeger, J.C. and Munroe, R.J., 1976, Heat flow and near-surface radioactivity in the Australian continental crust, *United States Department of the Interior, Geological Survey, Open-File Report*, 76–250.

[6] Middleton, M.F., 1979. Heat flow in the Moomba, Big Lake and Toolachee gas fields of the Cooper Basin and implications for hydrocarbon maturation, (Bull. Aust. Soc.) *Exploration Geophysics*, 10, 149–155.

[7] Beardsmore, G.R. and Cull, J.P., 2001, Crustal Heat Flow, A Guide to Measurement and Modelling, Cambridge University Press, 2001, 324p, ISBN 978-0-521-79703-0.

[8] Chopra, P.N, and Holgate, F., 2005, A GIS analysis of temperature in the Australian crust, *Proceedings of the World Geothermal Congress 2005*, Antalya, Turkey, 24–29 April 2005, 1–7.

[9] Budd, A.R., 2011, Geothermal Energy Project, Mapping Heat Across the Australian Continent, 3rd Hot Rock Energy Conference 2011.

[10] Budd, A.R., Gerner, E., Meixner, A.J., Kirkby, A.I., Weber, R. and Spring, J., 2011, Geoscience Australia's onshore energy security program: geothermal energy, in: *Proceedings of the 2011 Australian Geothermal Energy Conference*, 16–18 November, Melbourne, Geoscience Australia, Record 2011/43, (Budd, A.R. Ed.), 31–36.

[11] Bestow, T.T., 1982, The potential for geothermal energy in Western Australia, *Geological Survey of Western Australia*, Record 82/6. 67p.

[12] Ghori, K.A.R., 2009, Petroleum data: leading the search for geothermal resources in Western Australia, *APPEA Journal*, 365–382.

[13] Reid, P. W., Messeiller M., Llanos E. M. and Hasting, M., 2011, Paralana 2 – Well Testing and Stimulation Australian Geothermal Energy Conference 2011, Geoscience Australia Record 2011/43, (A. Budd, Ed.), 193–196.

[14] Cull, J.P. and Denham, D., 1979, Regional variations in Australian heat flow, *BMR Journal of Australian Geology and Geophysics*, 4, 1–13.

[15] Cull, J.P., 1982, An appraisal of Australian heat flow data, *BMR Journal of Australian Geology and Geophysics*, 7, 11–21.

[16] Middleton, M.F., 2013, Radiogenic heat generation in the Darling Range, Western Australia, *Exploration Geophysics*, 44, 206–214.

[17] Middleton, M. F. and Stevens, M.K.S., 2014, Heat Generation in the Vasse Shelf Region: Implications for Geothermal Exploration, Petroleum in Western Australia, March issue 2014.

[18] Middleton, M.F., 2014, Brett, J. and Flint, D., 2014, Thorium occurrence: geological and geophysical implications for Western Australia, Chapter 6. In: Thorium: Chemical Properties, Uses and Environmental Effects, (R. Jamison, Ed.) Nova Science Publishers Inc., ISBN: 978-1-63321-309-8, pp. 133–178.

[19] Brett, J, 2013, *Thorium merge map of WA, Geological Survey of Western Australia,* electronic publication.

[20] Minty, B.R.S., 1997, Fundamentals of airborne gamma-ray spectrometry, AGSO *Journal of Australian Geology and Geophysics*, v. 17, No. 2, 39–50.

[21] Minty, B., 2014, The Gamma-ray Spectrometric Method for Mineral Exploration and Environmental Mapping, ASEG OzSTEP Workshop2014.

[22] Minty, B., Franklin, R., Milligan, P., Richardson, L.M. and Wilford, J., 2009, The radiometric map of Australia, *Exploration Geophysics*, 40, 325–333.

[23] Kappelmeyer, O. and Haenel, R., 1974, Geothermics with Special Reference to Application, Bebrüder Borntraeger.

[24] Carslaw, H.S. and Jaeger, J.C., 1959, Conduction of Heat in Solids, Oxford University Press.

[25] Jessop, A.M., 1990, Thermal Geophysics, Developments in Solid Earth Geophysics, Elsevier, Amsterdam, 306p.

[26] Ryback, L., 1986, Amount and significance of radioactive heat sources in sediments. In: Thermal Modelling in Sedimentary Basins, Collections Colloques et Seminaires (J. Burrus, Ed.) 44, Editions Technip, Paris.

[27] Bücker, C. and Ryback, L., 1996, A simple method to determine heat production from gamma-ray logs, *Marine and Petroleum Geology*, 13, 373–375.

[28] SPE, 2015, http://petrowiki.org/Gamma_ray_logs.

[29] Crostella, A., and Backhouse J., 2000, Geology and petroleum exploration of the central and southern Perth Basin, Western Australia: *Western Australia Geological Survey, Report 57*, 85p.

[30] Cockbain, A.E., Hocking, R.M. and Myers, J.S., 1990, Geological Evolution, Phanerozoic, in *Geology and Mineral Resources of Western Australia*, *Western Australia Geological Survey*, Memoir *3*, 735–755.

[31] Middleton, M.F., Wilde, S.A., Evans, B.J., Long, A., Dentith, M. and Morawa, 1995, Deep seismic reflection traverse over the Darling Fault Zone, Western Australia, *Australian Journal of Earth Science*, 42, 83–93.

[32] Iasky, R. P., 1993, A structural study of the southern Perth Basin, Western Australia: *Western Australia Geological Survey, Report 31*.

[33] Mory, A.J. and Iasky, R.P., 1996, Stratigraphy and structure of the onshore Perth Basin, Western Australia: *Western Australia Geological Survey, Report 46*.

[34] Middleton, M.F., 2011, Temperatures within outcropping, radiogenic granites: Implications for geothermal energy in Western Australia, in: Middleton, M. and Gessner, K. (Eds) *West Australian Geothermal Energy Symposium Abstracts*, 21 & 22 March 2011, v. 1, 20 (ISBN 978-1-74052-230-41.

[35] Hot Dry Rocks, 2008, Geothermal energy potential in selected areas of Western Australia (Perth Basin), a report prepared for the Department of Industry and Resources, Western Australia. *Geological Survey of Western Australia, Statutory Petroleum Exploration Report*, G31888 A2.

[36] Schön, J.H., 1996, Physical Properties of Rocks: Fundamentals and Principles of Petrophysics, Pergamon.

[37] Wharton, P.H., 1982, The geology and hydrogeology of the Quindalup boreline, southern Perth Basin, Western Australia, *Geological Survey of Western Australia*, Record 1982/2.

[38] Playford, P. E., Cockbain, A. E. and Low, G. H., 1976, Geology of the Perth Basin, Western Australia: *Western Australia Geological Survey*, *Bulletin* 124.

[39] Wilde, S.A., Middleton, M.F. and Evans, B.J., 2006, Terrane accretion in the southwestern Yilgarn Craton: evidence from a deep seismic crustal profile, *Precambrian Research*, 78, 179–196.

[40] Annand, R.R. and Butt, C.R.M., 2003, Distribution and evolution of 'laterites' and lateritic weathering profiles, Darling Range, Western Australia, *Australian Geomechanics*, v. 36, No. 4, 41–58.

[41] Middleton, M.F., 2010, The Gillingarra temperature anomaly, northern Perth Basin, Australia, *Expanded Abstracts, Proceedings of SEG International Exposition and 80th Annual Meeting, Denver, Colorado*, October 2010.

[42] Regenauer-Lieb, K. and the Team of the Western Australian Centre of Excellence, 2011, Geothermal Cities, Australian Geothermal Energy Conference 2011, Geoscience Australia Record 2011/43, (A. Budd, Ed.), 185–188.

[43] Regenauer-Lieb, K. and the Team of the Western Australian Centre of Excellence, 2012, The Western Australian Geothermal Research Centre and its future, in: Middleton, M. and Gessner, K. (Eds) *West Australian Geothermal Energy Symposium Abstracts*, 2 & 3 April 2012, v. 2, 23–24 (ISBN 978-1-74052-250-2.

[44] Schilling, O, Sheldon, H.A., Reid, L.B. and Corbel, S., 2013, Hydrothermal models of the Perth metropolitan area, Western Australia: implications for geothermal energy, *Hydrogeology Journal* 21 (3), 605–621.

[45] Ballesteros, M., 2012, personal communication, concerning geothermal developments in the Perth metropolitan area.

[46] Pujol, M., Ricard, L., and Bolton, G., 2015, 20 years of exploitation of the Yarragadee aquifer in the Perth Basin of Western Australia for direct-use geothermal heat, *Geothermics*, v. 57, 39–55.

[47] Ricard, L and Pujol, M., 2015, Geothermal production in the Perth Metropolitan Area, 20 years of success. Petroleum in Western Australia, September issue, 2015.

[48] Hocking, R. M., van de Graaff., W. J. E., Blockley, J. G. and Butcher, B.P., 1982. Ajana, W.A.: *Western Australia Geological Survey*, 1:250 000 Geological Series Explanatory Notes.

[49] Ghori, K.A.R. and Gibson, H., 2011, Geothermal simulation, Perth Basin, Western Australia, in: 2011, *Proceedings of the 2011 Australian Geothermal Energy Conference*, 16–

18 November, Melbourne, Geoscience Australia, Record 2011/43, (A. Budd, Ed.), 77–80.

[50] Sanders, A. J. and McGuiness, S. A., 2000, Geochemical mapping of the Ajana 1:250 000 map sheet: *Western Australia Geological Survey*, 1:250 000 Regolith Geochemistry Series Explanatory Notes, 55p.

[51] Ghori, K.A.R., 2008, Perth Basin's geothermal resources, *Australian Geothermal Energy Conference 2008, Extended Abstracts*, 55–61.

[52] Van Krandendonk, M.J., Smithies, R. H., Hickman, A.H. and Champion, D.C., 2007, Review: secular tectonic evolution of Archean continental crust: interplay between horizontal and vertical processes in the formation of the Pilbara Craton, Australia, *Terra Nova*, 19, 1–28.

[53] Van Krandendonk, M.J., 2011, Personal communication concerning the geochemical database of the Geological Survey of Western Australia.

[54] Welch, P. and Boyle, P., 2009, New turbines to enable efficient geothermal power plants, *Geothermal Research Council (GRC) Transactions*, 33, 765–772.

[55] Welch, P., Boyle, P., Sells, M. and Murillo, I., 2010, Performance of new turbines for geothermal power plants, *Geothermal Research Council (GRC) Transactions*, 34, 1091–1096.

[56] Middleton, M.F., 2013, Implications of high heat flow and temperatures for geothermal energy in the southern Carnarvon Basin, Petroleum in Western Australia, April issue 2013. Hot Dry Rocks, 2009, Geothermal Energy Potential in Selected Areas of Western Australia (Canning Basin), a report prepared for the Department of Mines and Petroleum, *Western Australia Report* DOIR0681008.

[57] Davidson. C., Anderson, T. and Stanley, D.R, 2011, Development of Geothermal Waters for Recreational Purposes – Mornington Peninsula Australia, Australian Geothermal Energy Conference 2011, Geoscience Australia Record 2011/43, (A. Budd, Ed.), 49–52.

[58] Davidson, C., 2012, Geothermal beyond power – Opportunities for geothermal resource development, West Australian Geothermal Energy Symposium, Abstracts 2012, 2–3 April 2012, (M. Middleton and K. Gessner, Eds), ISBN 978-1-74052-250-2, p. 4.

[59] Hocking, R. M., Moors, H. T. and van de Graaff. W. J. E., 1987, Geology of the Carnarvon Basin, Western Australia: *Western Australia Geological Survey*, Bulletin 133.

[60] Hocking, R., 1990, The Carnarvon Basin, in Geology and Mineral Resources of Western Australia, *Western Australia Geological Survey*, Memoir 3, 457–495.

[61] Malcolm, R.J., Pott, M.C. and Delfos, E., 1991, A new tectono-stratigraphic synthesis of the North West Cape area, *APEA Journal*, 31, 154–176.

[62] Lennard, E.L., 1991, YALLINGUP SHEET 1930 IV and part Sheet 18301, Geological Survey of Western Australia. 1:50 000 Environmental Geology Series.

IntechOpen